

Transport and optical conductivity in dilute magnetic semiconductors

This article has been downloaded from IOPscience. Please scroll down to see the full text article.

2009 J. Phys.: Condens. Matter 21 084202

(<http://iopscience.iop.org/0953-8984/21/8/084202>)

View [the table of contents for this issue](#), or go to the [journal homepage](#) for more

Download details:

IP Address: 129.252.86.83

The article was downloaded on 29/05/2010 at 17:57

Please note that [terms and conditions apply](#).

Transport and optical conductivity in dilute magnetic semiconductors

F V Kyrychenko and C A Ullrich

Department of Physics and Astronomy, University of Missouri, Columbia, MO 65211, USA

Received 11 August 2008, in final form 7 October 2008

Published 30 January 2009

Online at stacks.iop.org/JPhysCM/21/084202

Abstract

A theory of transport in spin and charge disordered media is developed, with a particular emphasis on dilute magnetic semiconductors. The approach is based on the equation of motion for the current–current response function and considers both spin and charge disorder and electron–electron interaction on an equal footing. The formalism is applied to the specific case of $\text{Ga}_{1-x}\text{Mn}_x\text{As}$. Within the single parabolic band approximation it is shown that both spin (p – d exchange) and charge (Coulomb) scattering contributions to the resistivity are of the same order of magnitude and should be treated simultaneously. Positional correlations of charged impurities are shown to significantly increase the Coulomb scattering. In the magnetically ordered phase, the suppression of localized spin fluctuations leads to a sizable reduction of spin scattering, which may contribute to the experimentally observed drop in resistivity below the critical temperature. The developed model allows for a comprehensive treatment of electron–electron interaction, screening and correlation effects by means of time-dependent density-functional theory. It is shown that collective modes and a dynamical treatment of electron–electron interaction are essential for an accurate description of the infrared absorption spectrum.

(Some figures in this article are in colour only in the electronic version)

1. Introduction

The idea of utilizing the carrier spins in new electronic devices provides the basis for the rapidly developing field of spintronics [1]. A unique combination of magnetic and semiconducting properties makes dilute magnetic semiconductors (DMSs) attractive for various spintronics applications [2]. One of the most remarkable features of these materials is the onset of carrier-mediated ferromagnetism, potentially allowing us to control the spin degree of freedom by means of externally applied electric fields. A lot of attention is drawn to $\text{Ga}_{1-x}\text{Mn}_x\text{As}$ since the discovery of its relatively high ferromagnetic transition temperature [2], with a current record of $T_c = 159$ K [3].

It is generally believed [4] that the properties of the narrow-gap DMSs like $\text{In}_{1-x}\text{Mn}_x\text{As}$ are well described by models based on the band structure of the host material, while in wider-gap DMSs like $\text{Ga}_{1-x}\text{Mn}_x\text{N}$ and $\text{Ga}_{1-x}\text{Mn}_x\text{P}$ the itinerant carriers reside within narrow impurity bands, which drastically affects the electronic and transport properties of these systems.

Unlike other III–V DMSs, the nature of itinerant carriers in $\text{Ga}_{1-x}\text{Mn}_x\text{As}$ is still a subject of intense debate. The

valence band picture has been widely used [5], but recent experimental results [6, 7] suggest that the carriers might instead reside in an impurity band (for an alternative interpretation of these experimental results, see [8]). First-principles calculations [9, 10] have not been fully conclusive regarding the nature of the itinerant carriers. Therefore, a lot of attention is being paid to effective Hamiltonian models [11, 12] (whether based on the host band structures or impurity bands) or Monte Carlo simulations [13] and their abilities to adequately describe the experimental results.

Most studies of transport and optical conductivity within the host material valence band picture in $\text{Ga}_{1-x}\text{Mn}_x\text{As}$ treat the band structure in detail, while disorder and many-body effects are only accounted for using simple phenomenological relaxation time approximations and static screening models [14, 15]. On the other hand, the sensitivity of magnetic and transport properties of $\text{Ga}_{1-x}\text{Mn}_x\text{As}$ to details of the growth conditions [16] and post-growth annealing [17–19] points to the crucial role played by the defects and their configurations, and has stimulated intense research on the structure of defects and their influence on the various properties of the system [20]. It is essential, therefore, to develop a theory

of electrical conductivity in DMSs with more emphasis given to disorder and electron–electron correlations.

Here we present a theory for the electron dynamics in DMSs, taking into account the electronic band structure of the semiconductor host material combined with first-principles descriptions of disorder and many-body effects. Our approach is based on the equation of motion for the paramagnetic current response function and has some similarities to models developed earlier using the so-called memory function formalism [21–23]. The advantage of our approach as compared to the memory function formalism [21] is the simplicity and transparency of the derivation and the straightforward possibility to include the spin degree of freedom. Our formalism not only goes beyond the simple relaxation time approximation for disorder scattering, but also allows us to consider key features of DMSs such as spin and charge disorder and electron–electron interaction on an equal footing. The approach is able to account for correlations between impurity positions and between fluctuations of localized spins. The many-body effects are treated via time-dependent density-functional theory [24], which enables us to capture dynamic screening and collective electronic excitations of the itinerant carriers in principle exactly.

A preliminary account of our approach has been recently given in [25]. In the following, we shall provide a detailed derivation of the main formalism and give some new results regarding the effects of magnetic ordering in DMSs on their transport properties. We shall limit ourselves here to describing the host semiconductor using a simplified model with a single parabolic band. While this model has obvious limitations, it has the advantage that the derivations are more transparent than in a multiband case, while the essential physics (for instance, the effects of impurity correlations, or of collective electronic modes) are captured at least qualitatively correctly.

This paper is organized as follows. In section 2 we present the general theory of electronic transport in spin and charge disordered media. Then we apply our formalism to describe specific cases of interest in $\text{Ga}_{1-x}\text{Mn}_x\text{As}$. In section 3 we consider magnetically ordered systems and estimate the effect of the suppression of the localized spin fluctuations on the conductivity. In section 4 we investigate the role of positional and orientational correlations of scattering centers on the transport properties of $\text{Ga}_{1-x}\text{Mn}_x\text{As}$. Section 5 is devoted to the issue of dynamical screening and collective excitations in DMSs like $\text{Ga}_{1-x}\text{Mn}_x\text{As}$ and their importance for an adequate description of experimental results in the mid-infrared absorption range.

2. General theory

2.1. Current–current response

Our goal is to calculate transport properties and optical response in spin and charge disordered materials. The Hamiltonian of such a system in an electromagnetic field can be schematically represented as

$$\hat{H}_A = \frac{1}{2m} \sum_i \left(\hat{\mathbf{p}}_i + \frac{e}{c} \mathbf{A}(\mathbf{r}_i, t) \right)^2 + U(\mathbf{r}_1, \dots, \mathbf{r}_N), \quad (1)$$

where the potential U , discussed in more detail below, includes electron–electron interaction, charge disorder and localized magnetic impurities.

The most general approach in spin-dependent systems is to work with spin-current matrices, which allows one to describe the spin-resolved response and perturbations coupling to spin. However, in the following we shall only consider situations where we apply a spin-independent perturbation and measure its effect on spin-independent quantities. In this case it is sufficient to consider the spin-independent total current, defined as

$$\hat{\mathbf{j}}(\mathbf{r}) = \frac{1}{2} \sum_i (\hat{\mathbf{v}}_i \delta(\mathbf{r} - \mathbf{r}_i) + \delta(\mathbf{r} - \mathbf{r}_i) \hat{\mathbf{v}}_i), \quad (2)$$

where the summation is performed over all electrons and $\hat{\mathbf{v}}_i$ is the time-dependent electron velocity, whose components are given by

$$\hat{v}_i^\alpha = \frac{i}{\hbar} [\hat{H}_A, \hat{x}_i^\alpha] = \frac{1}{m} \left(\hat{p}_i^\alpha + \frac{e}{c} A_\alpha \right). \quad (3)$$

The above expression is derived under the assumption that the potential energy in equation (1) does not depend on momentum. If it does (e.g. in the case of spin–orbit interaction), expression (3) should be modified. If U includes the crystal potential, then m would be the free-electron mass. If, however, the crystal potential is implicit in the band structure then m here stands for an effective mass. In this derivation it is also assumed that the effective mass is energy-independent, so equation (3) is valid only for parabolic dispersions. Otherwise, the effective mass becomes a function of momentum and thus does not commute with the position operator any more, which would require a more careful treatment.

Assuming that the external electromagnetic field is weak, the Hamiltonian (1) can be linearized and becomes

$$\hat{H}_A \approx \hat{H} + \frac{e}{c} \int_V \hat{\mathbf{j}}_p(\mathbf{r}) \mathbf{A}(\mathbf{r}, t') e^{i\eta t'} d\mathbf{r}, \quad (4)$$

where we include the usual adiabatic switching factor $e^{i\eta t'}$, and the vector potential \mathbf{A} is coupled to the paramagnetic part of total current (2):

$$\hat{\mathbf{j}}_p(\mathbf{r}) = \frac{1}{2m} \sum_i (\hat{\mathbf{p}}_i \delta(\mathbf{r} - \mathbf{r}_i) + \delta(\mathbf{r} - \mathbf{r}_i) \hat{\mathbf{p}}_i). \quad (5)$$

The unperturbed Hamiltonian \hat{H} is time-independent, but contains disorder.

Within the linear response, the induced current averaged over the perturbed Hamiltonian (1) is given by

$$\langle \hat{j}_\alpha^{(1)}(\mathbf{q}, \omega) \rangle_A = \sum_\beta \sum_{\mathbf{q}'} \left(\frac{n}{m} \delta_{\alpha\beta} \delta_{\mathbf{q}\mathbf{q}'} + \chi_{J_{p\alpha} J_{p\beta}}(\mathbf{q}, \mathbf{q}', \omega) \right) \frac{e}{c} A_\beta(\mathbf{q}', \omega), \quad (6)$$

where $\alpha, \beta = x, y, z$ are Cartesian coordinates, n is the particle density and $\chi_{J_{p\alpha} J_{p\beta}}(\mathbf{q}, \mathbf{q}', \omega)$ is the Fourier transform of the paramagnetic current–current response function:

$$\chi_{J_{p\alpha} J_{p\beta}}(\mathbf{r}, \mathbf{r}', \tau) = -\frac{i}{\hbar} \Theta(\tau) \langle [\hat{J}_{p\alpha}(\tau, \mathbf{r}), \hat{J}_{p\beta}(\mathbf{r}')] \rangle_H. \quad (7)$$

The disorder enters equation (7) implicitly through the time evolution of the paramagnetic current operators, which is governed by the full system Hamiltonian \hat{H} . To get this dependence explicitly we will use the equation of motion for the paramagnetic current response function. First, however, we need to establish the form of the full system Hamiltonian \hat{H} .

2.2. Hamiltonian and four-component vectors

We represent the unperturbed Hamiltonian \hat{H} from equation (4) as the sum of a ‘clean’ and a disordered part:

$$\hat{H} = \hat{H}_c + \hat{H}_d, \quad (8)$$

where the clean part of the Hamiltonian includes electron and magnetic subsystem contributions:

$$\hat{H}_c = \hat{H}_e + \hat{H}_m. \quad (9)$$

The electron part \hat{H}_e involves band operators while the magnetic ion part \hat{H}_m contains only localized spin operators, whereas the disorder Hamiltonian \hat{H}_d contains both types of operators. Therefore, \hat{H}_e and \hat{H}_m commute with each other, but neither of them commute with \hat{H}_d .

For spin-dependent disorder potentials we use the general expression

$$\begin{aligned} \hat{H}_d &= \sum_i \sum_j \left(U_0(\mathbf{r}_i - \mathbf{R}_j) + \hat{U}_j(\mathbf{r}_i - \mathbf{R}_j) \cdot \vec{\sigma}_i \right) \\ &= V^2 \sum_{\mathbf{q}} \left(U_c(\mathbf{q}) \hat{n}(-\mathbf{q}) + \hat{U}(\mathbf{q}) \cdot \hat{\mathbf{s}}(-\mathbf{q}) \right), \end{aligned} \quad (10)$$

where $\hat{n}(-\mathbf{q})$ and $\hat{\mathbf{s}}(-\mathbf{q})$ are the charge- and spin-density operators of the band carriers, and the charge and spin disorder potentials are given by

$$U_c(\mathbf{q}) = U_0(\mathbf{q}) n_I(\mathbf{q}) = U_0(\mathbf{q}) \frac{1}{V} \sum_j e^{-i\mathbf{q} \cdot \mathbf{R}_j} \quad (11)$$

and

$$\hat{U}(\mathbf{q}) = \frac{1}{V} \sum_j \hat{U}_j(\mathbf{q}) e^{-i\mathbf{q} \cdot \mathbf{R}_j}. \quad (12)$$

The index j in the spin-dependent potential \hat{U}_j reflects the possibility of different values of this potential at different sites (orientational degree of freedom of localized spins). For Coulomb scatterers we assume identical potentials at all sites \mathbf{R}_j .

Let us now introduce a four-component vector:

$$\hat{\rho} = \begin{pmatrix} \hat{\rho}^1 \\ \hat{\rho}^+ \\ \hat{\rho}^- \\ \hat{\rho}^z \end{pmatrix} = \begin{pmatrix} \hat{n} \\ \hat{s}^+ \\ \hat{s}^- \\ \hat{s}^z \end{pmatrix} \quad (13)$$

whose components are the band carriers charge- and spin-density operators. Using the Pauli matrices

$$\begin{aligned} \sigma^1 &= \begin{pmatrix} 1 & 0 \\ 0 & 1 \end{pmatrix}, & \sigma^+ &= \begin{pmatrix} 0 & 1 \\ 0 & 0 \end{pmatrix}, \\ \sigma^- &= \begin{pmatrix} 0 & 0 \\ 1 & 0 \end{pmatrix}, & \sigma^z &= \begin{pmatrix} 1 & 0 \\ 0 & -1 \end{pmatrix}, \end{aligned} \quad (14)$$

the components of vector (13) can be expressed in a uniform way as

$$\hat{\rho}^i(\mathbf{q}) = \frac{1}{V} \sum_{\mathbf{k}} \sum_{\mu, \nu} (\sigma^i)_{\mu\nu} \hat{a}_{\mathbf{k}-\mathbf{q}, \mu}^+ \hat{a}_{\mathbf{k}, \nu}, \quad (15)$$

and the disorder Hamiltonian (10) takes on the compact form

$$\hat{H}_d = V^2 \sum_{\mathbf{q}} \hat{U}(\mathbf{q}) \cdot \hat{\rho}(-\mathbf{q}). \quad (16)$$

Here, we have introduced a four-component (one for charge and three for spin) potential vector \hat{U} , whose components are either c numbers or operators that are linear in the spin of the magnetic ions.

2.3. Equation of motion for the response function

In this section we highlight the main steps of the derivation of the equation of motion and discuss the various approximations involved.

The time derivative of the paramagnetic current response function (7) is given by

$$\begin{aligned} \frac{\partial}{\partial \tau} \chi_{j_{p\alpha} j_{p\beta}}(\mathbf{q}, \mathbf{q}', \tau) &= -\frac{i}{\hbar} \delta(\tau) V \langle [j_{p\alpha}(\mathbf{q}), j_{p\beta}(-\mathbf{q}')] \rangle_H \\ &\quad - \chi_{j_{p\alpha} F_{\beta}}(\mathbf{q}, \mathbf{q}', \tau), \end{aligned} \quad (17)$$

where $\hat{F}_{\alpha}(\mathbf{q}, \tau)$ is the α th component of the driving force:

$$\begin{aligned} \hat{F}_{\alpha}(\mathbf{q}, \tau) &= \frac{\partial}{\partial \tau} \hat{j}_{p\alpha}(\mathbf{q}, \tau) = -\frac{i}{\hbar} [\hat{j}_{p\alpha}(\mathbf{q}, \tau), \hat{H}] \\ &= \hat{F}_{\alpha}^c(\mathbf{q}, \tau) + \hat{F}_{\alpha}^d(\mathbf{q}, \tau), \end{aligned} \quad (18)$$

which we split into its clean and fluctuating (disordered) parts. The fluctuating part of the driving force can be immediately calculated as

$$\begin{aligned} \hat{F}_{\alpha}^d(\mathbf{q}, \tau) &= -\frac{i}{\hbar} e^{\frac{i}{\hbar} \hat{H} \tau} [\hat{j}_{p\alpha}(\mathbf{q}), \hat{H}_d] e^{-\frac{i}{\hbar} \hat{H} \tau} \\ &= -\frac{iV}{m} \sum_{\mathbf{q}'} q'_{\alpha} \hat{U}(\mathbf{q}', \tau) \cdot \hat{\rho}(\mathbf{q} - \mathbf{q}', \tau). \end{aligned} \quad (19)$$

The first approximation we use is the assumption that the main effect of disorder is due to the fluctuating part of the driving force, and in the time evolution of the clean part we can therefore approximate $\hat{H} \approx \hat{H}_c$:

$$\begin{aligned} \hat{F}_{\alpha}^c(\mathbf{q}, \tau) &= -\frac{i}{\hbar} e^{\frac{i}{\hbar} \hat{H}_c \tau} [\hat{j}_{p\alpha}(\mathbf{q}), \hat{H}_c] e^{-\frac{i}{\hbar} \hat{H}_c \tau} \\ &\approx -\frac{i}{\hbar} e^{\frac{i}{\hbar} \hat{H}_c \tau} [\hat{j}_{p\alpha}(\mathbf{q}), \hat{H}_c] e^{-\frac{i}{\hbar} \hat{H}_c \tau} = \frac{\partial}{\partial \tau} \hat{j}_{p\alpha}^c(\mathbf{q}, \tau), \end{aligned} \quad (20)$$

where the superscript ‘c’ means that the time evolution of the operator is due to the clean part of the Hamiltonian only.

Under this approximation¹ the equation of motion can be presented in the form

$$\begin{aligned} \frac{\partial^2}{\partial \tau^2} \chi_{j_{p\alpha} j_{p\beta}}(\mathbf{q}, \mathbf{q}', \tau) &\approx \frac{\partial^2}{\partial \tau^2} \chi_{j_{p\alpha} j_{p\beta}}^c(\mathbf{q}, \mathbf{q}', \tau) \\ &\quad - \frac{\partial}{\partial \tau} \chi_{j_{p\alpha} F_{\beta}}^c(\mathbf{q}, \mathbf{q}', \tau) - \chi_{F_{\alpha} F_{\beta}}^c(\mathbf{q}, \mathbf{q}', \tau) \end{aligned}$$

¹ Note that if the single-band clean system Hamiltonian is diagonal in the plane wave basis $\hat{H}_c = \sum_{\mathbf{k}} \varepsilon(\mathbf{k}) \hat{a}_{\mathbf{k}}^+ \hat{a}_{\mathbf{k}}$, then a direct calculation shows that $[\hat{j}_{p\alpha}(0), \hat{H}_c] = 0$ and in the long-wavelength limit $\mathbf{q} \rightarrow 0$ our approximation thus becomes exact.

$$\begin{aligned}
 & + \frac{i}{\hbar} \delta(\tau) V \left(\langle [\hat{J}_{p\alpha}(\mathbf{q}), \hat{F}_{\beta}^i(-\mathbf{q}')] \rangle_H \right. \\
 & \left. - \langle [\hat{J}_{p\alpha}(\mathbf{q}), \hat{F}_{\beta}^i(-\mathbf{q}')] \rangle_{H_c} \right). \quad (21)
 \end{aligned}$$

Next, we assume our system to be macroscopically homogeneous. In clean homogeneous systems the response at point \mathbf{r} depends only on the distance $\mathbf{r} - \mathbf{r}'$ to the perturbation and not on the particular choice of points \mathbf{r} and \mathbf{r}' . Disorder obviously introduces nonhomogeneity in the system. If, however, the coherence length of the electrons is much shorter than the system size, summing over all electrons will leave us with an averaged effect of disorder that does not depend on the particular disorder configuration. For such macroscopically homogeneous systems the response function for operators \hat{A} and \hat{B} should also depend only on the distance $\mathbf{r} - \mathbf{r}'$. In other words

$$\chi_{AB}(\mathbf{q}, \mathbf{q}', \tau) \approx \delta_{\mathbf{q}, \mathbf{q}'} \chi_{AB}(\mathbf{q}, \tau). \quad (22)$$

The second term on the right-hand side of equation (21) vanishes for such homogeneous systems.

The third term is the fluctuating force–force response function:

$$\begin{aligned}
 \chi_{F_d^i F_{\beta}^i}(\mathbf{q}, \tau) &= \frac{iV}{\hbar} \Theta(\tau) \frac{V^2}{m^2} \sum_{\mathbf{k}\mathbf{k}'} k_{\alpha} k'_{\beta} \\
 &\times \left\langle \left[\hat{\mathcal{U}}(\mathbf{k}, \tau) \cdot \hat{\rho}(\mathbf{q} - \mathbf{k}, \tau), \hat{\mathcal{U}}(\mathbf{k}', \tau) \cdot \hat{\rho}(-\mathbf{q} - \mathbf{k}') \right] \right\rangle_H. \quad (23)
 \end{aligned}$$

We now apply a decoupling procedure with the idea to separate the above expression into parts containing only band carrier operators and only magnetic ion operators. To do so we assume for the moment that the interaction Hamiltonian \hat{H}_d in the time evolution exponent does not contain magnetic ion operators (they might be substituted, for example, by corresponding mean field values). As a result, the total Hamiltonian becomes a sum of two commuting parts: \hat{H}_m containing only localized spin operators and $\hat{H}_e + \hat{H}_d$ which involves only electron operators. The time evolution of $\hat{\mathcal{U}}(\mathbf{k}, \tau)$ is thus governed by \hat{H}_m and the time evolution of $\hat{\rho}(\mathbf{q} - \mathbf{k}, \tau)$ is due to $\hat{H}_e + \hat{H}_d$ only. Then, $\hat{\mathcal{U}}(\mathbf{k}, \tau)$ and $\hat{\rho}(\mathbf{q} - \mathbf{k}, \tau)$ commute with each other and the operator part of (23) becomes

$$\begin{aligned}
 & \left\langle \left[\hat{\mathcal{U}}(\mathbf{k}, \tau) \cdot \hat{\rho}(\mathbf{q} - \mathbf{k}, \tau), \hat{\mathcal{U}}(\mathbf{k}', \tau) \cdot \hat{\rho}(-\mathbf{q} - \mathbf{k}') \right] \right\rangle_H \\
 & \approx \sum_{\mu\nu} \left\{ \left\langle \hat{\mathcal{U}}_{\mu}(\mathbf{k}, \tau) \hat{\mathcal{U}}_{\nu}(\mathbf{k}') \right\rangle_{H_m} \right. \\
 & \times \left\langle \left[\hat{\rho}_{\mu}(\mathbf{q} - \mathbf{k}, \tau), \hat{\rho}_{\nu}(-\mathbf{q} - \mathbf{k}') \right] \right\rangle_{H_e + H_d} \\
 & + \left\langle \left[\hat{\mathcal{U}}_{\mu}(\mathbf{k}, \tau), \hat{\mathcal{U}}_{\nu}(\mathbf{k}') \right] \right\rangle_{H_m} \\
 & \times \left. \left\langle \hat{\rho}_{\nu}(-\mathbf{q} - \mathbf{k}') \hat{\rho}_{\mu}(\mathbf{q} - \mathbf{k}, \tau) \right\rangle_{H_e + H_d} \right\}. \quad (24)
 \end{aligned}$$

Equation (23) can now be written as

$$\begin{aligned}
 -\chi_{F_d^i F_{\beta}^i}(\mathbf{q}, \tau) &= -\frac{V^2}{m^2} \sum_{\mathbf{k}} \sum_{\mu\nu} k_{\alpha} k_{\beta} \left\langle \hat{\mathcal{U}}_{\mu}(\mathbf{k}, \tau) \hat{\mathcal{U}}_{\nu}(-\mathbf{k}) \right\rangle_{H_m} \\
 &\times \chi_{\rho^{\mu} \rho^{\nu}}(\mathbf{q} - \mathbf{k}, \tau) + \chi_A^{(3)}, \quad (25)
 \end{aligned}$$

where the first term originates from the first term on the right-hand side of equation (24) and the additional term $\chi_A^{(3)}$ is due to the second term.

As a result of the decoupling procedure, we ignore all the effects of the band carriers on the magnetic ion subsystem, such as magnetic polaron formation or carrier-mediated interaction between localized moments. These effects, however, can be partially restored by introducing an interaction between localized spins within \hat{H}_m , for instance with a phenomenological RKKY-type exchange constant. Note also that, while being a drastic approximation, the decoupling procedure concerns only the spin part of the formalism and has no effect whatsoever on the charge disorder treatment.

After decoupling, the time evolution of the localized spin operators is governed by the magnetic ion Hamiltonian \hat{H}_m . For noninteracting spins this time evolution is trivial and in the following we neglect it completely.

In the last term in equation (21) we apply the linear response formalism with respect to the disorder Hamiltonian \hat{H}_d , and after some algebra one obtains

$$\frac{V^2}{m^2} \delta(\tau) \sum_{\mathbf{k}} \sum_{\mu\nu} k_{\alpha} k_{\beta} \left\langle \hat{\mathcal{U}}_{\mu}(\mathbf{k}) \hat{\mathcal{U}}_{\nu}(-\mathbf{k}) \right\rangle_{H_m} \chi_{\rho^{\mu} \rho^{\nu}}^c(-\mathbf{k}) + \chi_A^{(4)}, \quad (26)$$

where $\chi_{\rho^{\mu} \rho^{\nu}}^c(-\mathbf{k})$ are the static response functions and the additional term $\chi_A^{(4)}$ has the same origin as the $\chi_A^{(3)}$ term in equation (25).

2.4. Final expression

Inserting equations (25) and (26) into equation (21) and performing the time Fourier transform $\int_{-\infty}^{\infty} \dots e^{i(\omega+i\eta)\tau} d\tau$, we obtain the final expression for the total current response function in the form

$$\begin{aligned}
 \chi_{\alpha\beta}^J(\mathbf{q}, \omega) &= \chi_{j_{p\alpha} j_{p\beta}}^c(\mathbf{q}, \omega) + \frac{n}{m} \delta_{\alpha\beta} \\
 &+ \frac{V^2}{m^2 \omega^2} \sum_{\mathbf{k}} k_{\alpha} k_{\beta} \sum_{\mu\nu} \left\langle \hat{\mathcal{U}}_{\mu}(\mathbf{k}) \hat{\mathcal{U}}_{\nu}(-\mathbf{k}) \right\rangle_{H_m} \\
 &\times \left(\chi_{\rho^{\mu} \rho^{\nu}}(\mathbf{q} - \mathbf{k}, \omega) - \chi_{\rho^{\mu} \rho^{\nu}}^c(-\mathbf{k}, 0) \right) + \chi^A, \quad (27)
 \end{aligned}$$

where the components of the second rank tensors χ and χ^c are the Fourier transforms of spin-density response functions:

$$\chi_{\rho^{\mu} \rho^{\nu}}(\mathbf{k}, \omega) = -\frac{iV}{\hbar} \int_0^{\infty} e^{i(\omega+i\eta)t} \langle [\hat{\rho}^{\mu}(\mathbf{k}, t), \hat{\rho}^{\nu}(-\mathbf{k})] \rangle_H dt. \quad (28)$$

χ^A stands for the sum of additional terms $\chi_A^{(3)} + \chi_A^{(4)}$ that result from the noncommutativity of the components of $\hat{\mathcal{U}}_{\mu}$. This term vanishes in paramagnetic systems and will be considered in more detail in section 3.

Equation (27) relates the current response function of the disordered system to the set of charge- and spin-density response functions of the disordered system. This expression is exact in the sense that it is valid regardless of the strength of disorder and, strictly speaking, should be calculated self-consistently. This approach was realized in [26] to study spin-independent systems close to the metal–insulator threshold. In our case, however, we assume that the disorder is weak enough so we can approximate equation (27) by expanding to second order in the disorder potential $\hat{\mathcal{U}}(\mathbf{k})$, and thus replace $\chi_{\rho^{\mu} \rho^{\nu}}(\mathbf{k}, \omega)$ by its clean system counterpart $\chi_{\rho^{\mu} \rho^{\nu}}^c(\mathbf{k}, \omega)$. In the following sections we apply our formalism to some specific situations in DMSs.

2.5. Multiband formalism

Before moving on, we briefly discuss a generalization of our model using a multiband treatment of the valence band hole states. The full system's current–current response is given by the general expression (27), where the multiband nature of the valence band enters via the response functions on the right-hand side of the equation. The current–current response of the clean system in the long-wavelength limit $q \rightarrow 0$ is given by

$$\begin{aligned} \chi_{j_{\alpha} j_{\beta}}^c(\omega) &= \frac{1}{Vm_0^2} \sum_{n,n',\mathbf{k}} \frac{f_{n',\mathbf{k}} - f_{n,\mathbf{k}}}{\varepsilon_{n',\mathbf{k}} - \varepsilon_{n,\mathbf{k}} + \hbar\omega + i\eta} \\ &\times \left[\sum_{s's} B_{s'}^*(n', \mathbf{k}) B_s(n, \mathbf{k}) \frac{m_0}{\hbar} \frac{\partial}{\partial k_{\alpha}} \langle s' | H_{\mathbf{k},\mathbf{p}} | s \rangle \right] \\ &\times \left[\sum_{s's} B_s^*(n, \mathbf{k}) B_{s'}(n', \mathbf{k}) \frac{m_0}{\hbar} \frac{\partial}{\partial k_{\beta}} \langle s | H_{\mathbf{k},\mathbf{p}} | s' \rangle \right], \quad (29) \end{aligned}$$

where the indices n, n' label different energy bands and $B_s(n, \mathbf{k})$ are the (complex) expansion coefficients corresponding to the s th basis function of the (n, \mathbf{k}) eigenvector of the multiband Hamiltonian $H_{\mathbf{k},\mathbf{p}}$.

Similarly, the components of the spin- and charge-density response tensor for multiband systems are given by

$$\begin{aligned} \chi_{\rho^{\mu} \rho^{\nu}}(\mathbf{q}, \omega) &= \frac{1}{V} \sum_{n,n',\mathbf{k}} \frac{f_{n',\mathbf{k}-\mathbf{q}} - f_{n,\mathbf{k}}}{\varepsilon_{n',\mathbf{k}-\mathbf{q}} - \varepsilon_{n,\mathbf{k}} + \hbar\omega + i\eta} \\ &\times \sum_{s',s,\tau,\tau'} B_{s'}^*(n', \mathbf{k}-\mathbf{q}) B_{\tau'}(n', \mathbf{k}-\mathbf{q}) B_s(n, \mathbf{k}) \\ &\times B_{\tau}^*(n, \mathbf{k}) \langle s' | \hat{\sigma}^{\mu} | s \rangle \langle \tau | \hat{\sigma}^{\nu} | \tau' \rangle, \quad (30) \end{aligned}$$

where the $\hat{\sigma}^{\mu}$ are Pauli matrices (14). Figure 1 shows the imaginary part of the long-wavelength limit of the current–current response function (29) (proportional to the real part of the conductivity), obtained within the standard eight-band $\mathbf{k} \cdot \mathbf{p}$ approach with the contribution of the remote bands taken into account up to second order in momentum. The sharp feature around 0.2 eV corresponds to the heavy-hole–light-hole inter-valence band transitions. The higher energy feature represent transitions from the split-off band to the heavy- and light-hole bands. The red dashed line in figure 1 includes the damping parameter $\eta \rightarrow \Gamma = 10$ meV to simulate the effects of inhomogeneous broadening and phonon scattering.

This work is currently in progress. Results of the calculations as well as a detailed derivation of the formalism in the multiband case will be presented elsewhere [32].

3. Effect of magnetic ordering

Magnetic ordering is known to have a strong effect on the transport properties of DMSs [27]. The resistivity of optimally annealed samples reveals a pronounced maximum at the ferromagnetic transition temperature T_c and decreases significantly for temperatures below T_c [28]. Lopez-Sancho and Brey [29] proposed to explain the resistivity change in terms of the variation of the Fermi surface and the transport scattering time when going from the paramagnetic to the ferromagnetic phase. Their model, however, completely neglects scattering off the fluctuations of localized spins. On

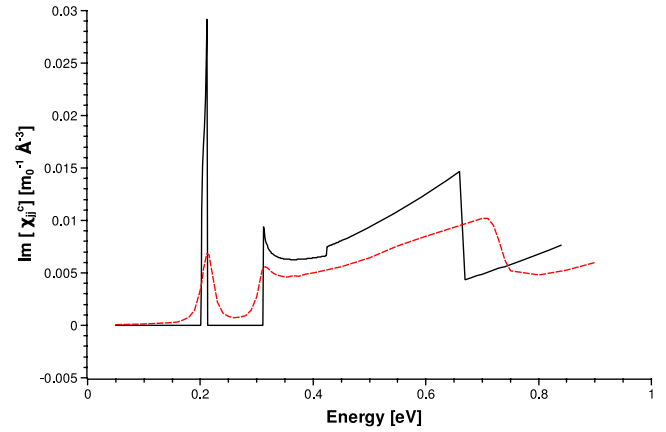


Figure 1. Imaginary part of the clean system current–current response function (29) for Ga_{0.95}Mn_{0.05}As, without (black) and with (red dashed) damping parameter to simulate inhomogeneous broadening.

the other hand, spin fluctuations are effectively suppressed in the ferromagnetic state. In the fully spin-polarized state scattering takes place only due to quantum fluctuations of the localized spins.

Before going into the calculations, however, we need to establish the explicit form of all expressions entering equation (27). Let us start with the disorder potential. In this section we will assume that only one type of disorder is present, namely Mn²⁺ ions randomly distributed in cation substitutional positions. The four-component vector of the disorder potential can then be written as

$$\hat{U}(\mathbf{k}) = \frac{1}{V} \sum_j \begin{pmatrix} U(\mathbf{k}) \\ \frac{J}{2} \hat{S}_j^- \\ \frac{J}{2} \hat{S}_j^+ \\ \frac{J}{2} (\hat{S}_j^z - \langle S \rangle) \end{pmatrix} e^{-i\mathbf{k} \cdot \mathbf{R}_j}, \quad (31)$$

where the summation is performed over all substitutional magnetic ions and $\hat{S}_j^{\pm} = \hat{S}_j^x \pm i\hat{S}_j^y$. Note that the mean field part of the p–d exchange interaction is absorbed in the electron part \hat{H}_e of the clean system Hamiltonian (9) and the spin part of the disorder potential consists of the fluctuations of localized spins around the mean field value. Specifically, the single-defect spin disorder operator in equation (12) is then

$$\hat{U}_j(\mathbf{q}) = \frac{J}{2} (\hat{S}_j - \langle S \rangle),$$

where we assumed a contact p–d interaction in the Heisenberg Hamiltonian, which results in a momentum-independent exchange constant J . In our calculations we use the value of $VJ = 55$ meV nm³, which corresponds to the widely used DMS p–d exchange constant $N_0\beta = 1.2$ eV [12]. In equation (31) and hereafter we choose the axis of quantization along the magnetization direction.

In principle, all effects of electron–electron interaction, including dynamic screening and collective excitations, are contained in equation (27) within the set of charge- and spin-density response functions of itinerant carriers $\chi_{\rho^{\mu} \rho^{\nu}}$. We will

study these effects in more detail in section 5. Here, we assume for simplicity that the role of the electron–electron interaction is reduced to the static screening of the Coulomb disorder potential. We approximate thus:

$$\chi_{nn}(\mathbf{q}, \omega) \approx \frac{\chi_{nn}^0(\mathbf{q}, \omega)}{\varepsilon_{\text{RPA}}(\mathbf{q}, 0)}, \quad (32)$$

where the static dielectric constant is [30]

$$\varepsilon_{\text{RPA}}(\mathbf{q}, 0) = 1 + \frac{q_{\text{TF}}^2}{2q^2} \left(1 + \frac{1-x^2}{2x} \ln \left| \frac{1+x}{1-x} \right| \right), \quad (33)$$

with $x = q/2k_F$ and $q_{\text{TF}} = \sqrt{\frac{6\pi e^2 n}{K E_F}}$ being the Thomas–Fermi wavevector. The charge component of the disorder vector (31) is now the bare acceptor potential (screened with the host material dielectric constant K):

$$U_n(q) = -\frac{1}{V} \frac{4\pi e^2}{K q^2}, \quad (34)$$

and the components of the spin- and charge-density response tensor $\chi_{\rho^\mu \rho^\nu}(q, \omega)$ are those for the noninteracting electron gas.

The derivation of the explicit form of the components of the response tensor is given in appendix A. Here we present the final expressions for the nonvanishing components of the tensor $\chi_{\rho^\mu \rho^\nu}$:

$$\begin{aligned} \chi_{nn}(\mathbf{q}, \omega) &= \chi_{s^z s^z}(\mathbf{q}, \omega) \\ &= -A_\uparrow^*(-\mathbf{q}, -\hbar\omega) - A_\uparrow(\mathbf{q}, \hbar\omega) \\ &\quad - A_\downarrow^*(-\mathbf{q}, -\hbar\omega) - A_\downarrow(\mathbf{q}, \hbar\omega), \end{aligned} \quad (35)$$

$$\begin{aligned} \chi_{s^z n}(\mathbf{q}, \omega) &= \chi_{ns^z}(\mathbf{q}, \omega) \\ &= -A_\uparrow^*(-\mathbf{q}, -\hbar\omega) - A_\uparrow(\mathbf{q}, \hbar\omega) \\ &\quad + A_\downarrow^*(-\mathbf{q}, -\hbar\omega) + A_\downarrow(\mathbf{q}, \hbar\omega), \end{aligned} \quad (36)$$

$$\begin{aligned} \chi_{s^+ s^-}(\mathbf{q}, \omega) &= \chi_{s^- s^+}(-\mathbf{q}, -\omega) \\ &= -A_\uparrow^*(-\mathbf{q}, -\hbar\omega - \Delta) - A_\downarrow(\mathbf{q}, \hbar\omega + \Delta). \end{aligned} \quad (37)$$

Here, Δ is the momentum-independent spin splitting (A.3), and the real and imaginary parts of $A_\sigma(\mathbf{q}, \omega)$ are given by equations (A.7) and (A.8). The derivation was performed for a degenerate hole gas assuming a simple parabolic dispersion for holes.

For magnetically ordered systems equation (27) contains an additional term χ_A that stems from the noncommutativity of the components of the disorder potential. This additional term is evaluated in appendix B and can be approximated as

$$\begin{aligned} \chi^A &\approx \frac{n_i V J^2}{2m^2 \omega^2} \langle S_z \rangle \sum_{\mathbf{k}} k_\alpha k_\beta (A_\uparrow(\mathbf{q} - \mathbf{k}, \hbar\omega - \Delta) \\ &\quad - A_\uparrow(k, -\Delta) - A_\downarrow(\mathbf{q} - \mathbf{k}, \hbar\omega + \Delta) + A_\downarrow(k, \Delta)). \end{aligned} \quad (38)$$

For the clean system described by the single-band Hamiltonian (A.1) direct evaluation gives $\chi_{j_{\text{pa}} j_{\text{pb}}}^c(\mathbf{q}, \omega) = 0$. Combining the obtained results, the total current response function (27) for spin and charge disordered system in spin-polarized state is

$$\chi_{\alpha\beta}^J(\mathbf{q}, \omega) = \frac{n}{m} \delta_{\alpha\beta} + \chi_{\alpha\beta}^n(\mathbf{q}, \omega) + \chi_{\alpha\beta}^s(\mathbf{q}, \omega), \quad (39)$$

where

$$\chi_{\alpha\beta}^n(\mathbf{q}, \omega) = \frac{n_i V}{m^2 \omega^2} \sum_{\mathbf{k}} k_\alpha k_\beta |U_n(k)|^2 \tilde{\chi}_{nn}(\mathbf{q} - \mathbf{k}, \omega) \quad (40)$$

and

$$\begin{aligned} \chi_{\alpha\beta}^s(\mathbf{q}, \omega) &= \frac{n_i V}{m^2 \omega^2} \frac{J^2}{4} \\ &\times \sum_{\mathbf{k}} k_\alpha k_\beta \left[\left(\langle \hat{S}_z^2 \rangle - \langle \hat{S}_z \rangle^2 \right) \tilde{\chi}_{s^z s^z}(\mathbf{q} - \mathbf{k}, \omega) \right. \\ &\quad + \langle \hat{S}^- \hat{S}^+ \rangle \tilde{\chi}_{s^+ s^-}(\mathbf{q} - \mathbf{k}, \omega) + \langle \hat{S}^+ \hat{S}^- \rangle \tilde{\chi}_{s^- s^+}(\mathbf{q} - \mathbf{k}, \omega) \\ &\quad \left. + 2 \langle \hat{S}_z \rangle \left(\tilde{A}_\uparrow(\mathbf{q} - \mathbf{k}, \hbar\omega - \Delta) - \tilde{A}_\downarrow(\mathbf{q} - \mathbf{k}, \hbar\omega + \Delta) \right) \right] \end{aligned} \quad (41)$$

are the contributions from the Coulomb and exchange scattering, respectively. We use a shorthand notation where \tilde{Q} indicates that the static part of a quantity Q is subtracted:

$$\tilde{Q}(\mathbf{q} - \mathbf{k}, \omega) \equiv Q(\mathbf{q} - \mathbf{k}, \omega) - Q(k, \omega = 0).$$

Spin and charge channels are separated in equation (39). This is a consequence of our model, where spin disorder consists of the fluctuations of localized spins around their mean field value. The first-order effects of spin disorder thus average to zero and the term proportional to the mixed spin–charge-density response $\chi_{s^z n}$ in equation (27) vanishes.

For optical response and conductivity we are mostly interested in the long-wavelength limit $\mathbf{q} \rightarrow 0$ of equation (39). In this case the current response tensor is proportional to a scalar $\chi_{\alpha\beta}^J = \chi^J \delta_{\alpha\beta}$. Although our approach is not a calculation of a relaxation time but rather is the evaluation of the full system current response, it is convenient to carry out the discussion in the familiar terms of energy- and momentum-dependent charge and spin relaxation rates. Comparing with the Drude expression in the weak disorder limit $\omega\tau \gg 1$,

$$\chi_D^J(\omega) = \frac{n}{m} \frac{1}{1 + i/\omega\tau} \approx \frac{n}{m} - \frac{in}{m\omega\tau},$$

we can express our results through charge and spin relaxation times τ_n and τ_s :

$$\chi^J(\omega) = \frac{n}{m} - \frac{in}{m\omega} \left(\frac{1}{\tau_n} + \frac{1}{\tau_s} \right), \quad (42)$$

with

$$\frac{1}{\tau_n(\omega)} = i \frac{n_i}{n} \frac{V^2}{6\pi^2 m \omega} \int_0^\infty k^4 |U_n(k)|^2 \tilde{\chi}_{nn}(k, \omega) dk, \quad (43)$$

and

$$\begin{aligned} \frac{1}{\tau_s(\omega)} &= i \frac{n_i}{n} \frac{V^2}{6\pi^2 m \omega} \frac{J^2}{4} \int_0^\infty k^4 \left[\left(\langle \hat{S}_z^2 \rangle - \langle \hat{S}_z \rangle^2 \right) \tilde{\chi}_{s^z s^z}(k, \omega) \right. \\ &\quad + \langle \hat{S}^- \hat{S}^+ \rangle \left(-\tilde{A}_\uparrow(k, \hbar\omega - \Delta) - \tilde{A}_\uparrow^*(k, -\hbar\omega - \Delta) \right) \\ &\quad \left. + \langle \hat{S}^+ \hat{S}^- \rangle \left(-\tilde{A}_\downarrow(k, \hbar\omega + \Delta) - \tilde{A}_\downarrow^*(k, -\hbar\omega + \Delta) \right) \right] dk. \end{aligned} \quad (44)$$

In figure 2 we present the temperature dependence of the total hole relaxation rate calculated according to equations (43)

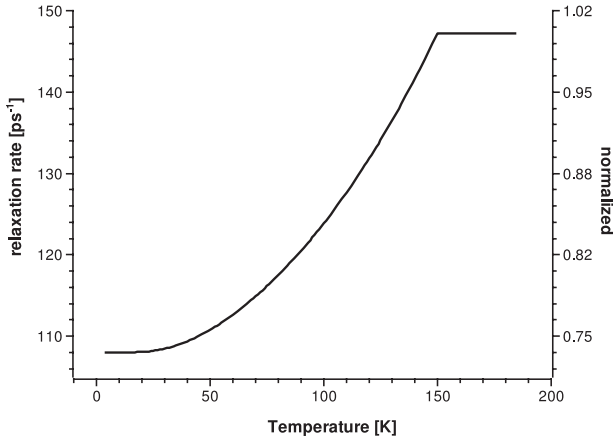


Figure 2. Temperature dependence of the total (charge and spin) carrier relaxation rate for $\text{Ga}_{0.95}\text{Mn}_{0.05}\text{As}$ with $T_c = 150$ K.

and (44) for $\text{Ga}_{0.95}\text{Mn}_{0.05}\text{As}$ with $T_c = 150$ K. In our calculations we used the standard mean field approach [31] to obtain the temperature dependence of the magnetization for the system with given critical temperature. Our calculations predict a 20–25% drop in resistivity in the ferromagnetic phase. This result is consistent with both experimental observations and the calculations of [29]. In our calculations, however, this result comes almost entirely from the spin relaxation (exchange scattering) channel. Suppression of localized spin fluctuations below T_c leads to a significant reduction of the spin relaxation rate from $\tau_s^{-1} = 60$ ps⁻¹ in the paramagnetic state to $\tau_s^{-1} = 20$ ps⁻¹ in the fully spin-polarized state. On the other hand, reference [29] completely neglects short-range exchange scattering and finds the 20% reduction of the Coulomb scattering to be due to changes of the Fermi surface in the ferromagnetic phase. The corresponding effect in our model is insignificant, which is likely due to the fact that in our calculations we used a simple parabolic band and isotropic spin splitting. Nevertheless, it is clear that the exchange scattering is not negligible in $\text{Ga}_{1-x}\text{Mn}_x\text{As}$. Further work that would consider both mechanisms including a comprehensive treatment of the valence band states [32] is required to adequately describe the experimentally observed drop in resistivity.

4. Correlations in impurity positions

The substitutional nature of Mn ions in the group III sublattices has been demonstrated by extended x-ray absorption fine structure (EXAFS) measurements of low-temperature MBE-grown samples [33, 34]. As for the spatial configuration of these defects, most theoretical models for transport in DMSs assume their random distribution. It was shown, however, both experimentally [35] and theoretically [36] that in samples with high Curie temperature the positions of substitutional magnetic ions are significantly correlated. These correlations originate from the interaction between magnetic impurities [37] and, in systems with strong compensation, are due to the presence of both positively and negatively charged defects. In the latter case, Timm *et al* [38] found in the limit of thermal equilibrium

that, driven by Coulomb attraction, the defects tend to form clusters. The main effect of such a clustering is *ionic* screening of the disorder Coulomb potential, which has been shown to be necessary to correctly reproduce the bandgap, metal–insulator transition and shape of the magnetization curve [38].

In this section, we apply our formalism to study the effect of the correlation of defect positions on electronic transport in DMSs. We show that the conductivity of $\text{Ga}_{1-x}\text{Mn}_x\text{As}$ is strongly modified through a momentum-dependent impurity structure factor. We will concentrate on heavily compensated systems where impurity structure factor effects are accompanied by ionic screening of the disorder potential.

In this case, the disorder Hamiltonian (16) is generalized to

$$\hat{H}_d = V^2 \sum_{\mathbf{k}} \left(\hat{U}^1(\mathbf{k}) + \hat{U}^2(\mathbf{k}) + \dots \right) \cdot \hat{\rho}(-\mathbf{k}), \quad (45)$$

where the $\hat{U}^i(\mathbf{q})$ describe different types of defects such as magnetic ions in cation substitutional positions (Mn_{Ga}), magnetic ions in interstitial positions (Mn_{I}) or arsenic antisite defects (As_{Ga}). For simplicity we will consider only two types of defects: magnetic ions in substitutional and interstitial positions. We will treat the latter as spinless double donors. The relation between the concentrations of acceptors and double donors is determined through the level of compensation p (number of holes per substitutional Mn ion). The product of the components of the disorder potential in equation (27), $\sum_{ii'} \langle \hat{U}_{\mu}^i(\mathbf{k}) \hat{U}_{\nu}^{i'}(-\mathbf{k}) \rangle_{H_m}$, has both diagonal ($i = i'$) and off-diagonal ($i \neq i'$) contributions. The product of the charge components of the off-diagonal donor–acceptor cross-term accounts for ionic screening in our model. We separate the product of two components of the disorder potential into contributions from the same defect and pairs of defects:

$$\begin{aligned} \langle \hat{U}_{\mu}^i(\mathbf{k}) \hat{U}_{\nu}^{i'}(-\mathbf{k}) \rangle_{H_m} &= \delta_{ii'} \frac{n_i}{V} \langle \hat{U}_{\mu}^i(\mathbf{k}) \hat{U}_{\nu}^i(-\mathbf{k}) \rangle_{H_m} \\ &+ \frac{1}{V^2} \sum_{\substack{j, j' \\ j \neq j'}} \langle \hat{U}_{\mu}^{ij}(\mathbf{k}) \hat{U}_{\nu}^{i'j'}(-\mathbf{k}) \rangle_{H_m} e^{i\mathbf{k} \cdot (\mathbf{R}_{j'}^i - \mathbf{R}_j^i)}. \end{aligned} \quad (46)$$

Note that the off-diagonal donor–acceptor cross-term with $i \neq i'$ does not contain the same-ion contribution. The summation over j and j' in equation (46) in this case involves substantially different defects and only the pair term is present.

4.1. Charge scattering

For the charge components $\mu = \nu = n$, equation (46) is

$$\begin{aligned} \langle \hat{U}_n^i(\mathbf{k}) \hat{U}_n^{i'}(-\mathbf{k}) \rangle_{H_m} &= U_n^i(\mathbf{k}) U_n^{i'}(-\mathbf{k}) \\ &\times \left(\delta_{ii'} \frac{n_i}{V} + \frac{1}{V^2} \sum_{j \neq j'} e^{i\mathbf{k} \cdot (\mathbf{R}_{j'}^i - \mathbf{R}_j^i)} \right) \\ &= U_n^i(\mathbf{k}) U_n^{i'}(-\mathbf{k}) \frac{n_i}{V} S_{ii'}(\mathbf{k}), \end{aligned} \quad (47)$$

where we have introduced a momentum-dependent impurity structure factor $S_{ii'}(\mathbf{k})$. A detailed analysis of the structure

factor is given in appendix C. The general expression has the form

$$S_{ii'}(\mathbf{k}) = \delta_{ii'} + \frac{n_{i'}V}{\Omega_0} \int_V P_{ii'}(R) \cos(\mathbf{k} \cdot \mathbf{R}) d\mathbf{R}, \quad (48)$$

where $P_{ii'}(R)$ is the pair correlation function. Note that the off-diagonal structure factor $S_{ii'}(\mathbf{k})$ with $i \neq i'$ vanishes for uncorrelated impurities. Therefore, the donor–acceptor cross-term, responsible for ionic screening of Coulomb disorder in our model, appears only if there are correlations in defect positions.

Correlated impurity positions give rise to a set of impurity structure factors in equation (43) for the charge relaxation rate. The generalized expression now is

$$\frac{1}{\tau_n(\omega)} = i \frac{V^2}{6\pi^2 m\omega} \int_0^\infty k^4 \times \left(\sum_{ii'} \frac{n_i}{n} U_n^i(k) U_n^{i'}(k) S_{ii'}(k) \right) \tilde{\chi}_{nn}(k, \omega) dk. \quad (49)$$

4.2. Spin scattering

It turns out that positional correlations alone are not sufficient to affect the exchange scattering. If any of the indices μ, ν in equation (46) is a spin index ($\mu = +, -, z$) then one finds for noninteracting spins

$$\begin{aligned} \left\langle \hat{U}_\mu^i(\mathbf{k}) \hat{U}_\nu^{i'}(-\mathbf{k}) \right\rangle_{H_m} &= \delta_{ii'} \frac{n_i}{V} \left\langle \hat{U}_\mu^i(\mathbf{k}) \hat{U}_\nu^{i'}(-\mathbf{k}) \right\rangle_{H_m} \\ &+ \frac{1}{V^2} \sum_{\substack{j, j' \\ j \neq j'}} \left\langle \hat{U}_\mu^{ij}(\mathbf{k}) \right\rangle_{H_m} \left\langle \hat{U}_\nu^{i'j'}(-\mathbf{k}) \right\rangle_{H_m} e^{i\mathbf{k} \cdot (\mathbf{R}_j - \mathbf{R}_{j'})} \end{aligned} \quad (50)$$

and the pair term vanishes in the paramagnetic state, regardless of the possible spatial correlations. This is a characteristic feature of spin scattering: there are two sources of randomness—spatial and orientational. In terms of scattering magnetic impurities are correlated only if there are correlations in both spatial positioning and momentum orientations. Orientational correlations, however, do not imply that the system has to be magnetically ordered. What counts in the scattering is the short-range orientational correlations that can be present even in a macroscopically paramagnetic system. We shall now consider this situation more closely.

During the decoupling procedure (24) we ignored the influence of band carriers on the localized magnetic moments. Among other processes we have neglected thus the carrier-mediated interaction between localized spins. To some extent we can restore this effect by introducing the interaction within the magnetic subsystem through the Heisenberg Hamiltonian:

$$\hat{H}_m = -\frac{1}{2} \sum_{j \neq j'} J_{jj'} \hat{\mathbf{S}}_j \cdot \hat{\mathbf{S}}_{j'} \quad (51)$$

with some phenomenological exchange constants $J_{jj'}$. It should be emphasized, however, that the localized spins in this approach remain decoupled from the itinerant carriers. Since we have completely neglected the time evolution of localized spins, the approximation should be viewed as an adiabatic approach where itinerant holes move through the ensemble of frozen localized spins.

We calculate the thermal average of the product of interacting spins in equation (46) within the high-temperature expansion [31]. Since we have only one type of defect that carries localized spins, namely Mn_{Ga} , there is only a diagonal term with $i = i'$ in the product of spin components, and in the following we drop this index for clarity. Details of the calculations and parameters used are presented in appendix D. The final expression for the product of spin components of disorder potential has the form

$$\begin{aligned} \left\langle \hat{U}_\mu(\mathbf{k}) \hat{U}_\nu(-\mathbf{k}) \right\rangle_{H_m} &= \delta_{\mu\nu} \frac{J^2 S(S+1) n_i}{4 \cdot 3} \frac{1}{V} S(\mathbf{k}), \\ \mu, \nu &= x, y, z, \end{aligned} \quad (52)$$

where the ‘orientational correlation adjusted’ structure factor $S(\mathbf{k})$ is

$$\begin{aligned} S(\mathbf{k}) &= 1 + \frac{2}{N_i} \frac{S(S+1)}{3} \sum_{j > j'} \frac{J_{jj'}(\mathbf{R}_{jj'})}{k_B T} \cos(\mathbf{k} \cdot \mathbf{R}_{jj'}) \\ &\approx 1 + N_i \frac{S(S+1)}{3k_B T} \frac{1}{\Omega_0} \int_V P(\mathbf{R}) J(\mathbf{R}) \cos(\mathbf{k} \cdot \mathbf{R}) d\mathbf{R}. \end{aligned} \quad (53)$$

The pair distribution function $P(\mathbf{R})$ is given by equation (C.5) and the effective exchange constant in Heisenberg Hamiltonian $J(\mathbf{R})$ is given by equation (D.3).

The modified expression for the spin scattering rate of the paramagnetic system with spatially correlated and interacting spins now is

$$\begin{aligned} \frac{1}{\tau_s(\omega)} &= i \frac{n_i}{n} \frac{V^2 J^2}{6\pi^2 m\omega} \frac{S(S+1)}{12} \int_0^\infty k^4 S(k) [\tilde{\chi}_{s^+s^-}(k, \omega) \\ &+ 2\tilde{\chi}_{s^+s^-}(k, \omega) + 2\tilde{\chi}_{s^-s^+}(k, \omega)]. \end{aligned} \quad (54)$$

4.3. Discussion

As for the Coulomb scattering, there are two competing effects associated with positional correlations of charge centers. One is the appearance of the momentum-dependent impurity structure factor that results in the enhancement of the scattering rate. The other is ionic screening, when the positive charge of donor compensating defects tends to screen the Coulomb disorder potential of the acceptor centers. There is no such effect as ionic screening for exchange scattering in our model, so for interacting spins their positional correlations should result in the increase of spin relaxation rate.

In figure 3 we plot the static ($\omega = 0$) relaxation rates (49) and (54) calculated as a function of the level of compensation for $\text{Ga}_{0.95}\text{Mn}_{0.05}\text{As}$. Thin lines correspond to randomly distributed defects. For heavily compensated systems (low number of holes per substitutional Mn ion) the Coulomb scattering dominates, while for cleaner systems due to the carrier screening of charge disorder the role of exchange scattering increases. Positional correlations in defects were modeled by clusters containing on average 10 Mn_{Ga} with effective concentration of substitutional Mn ions $x_c = 0.1$ within the cluster. The dashed line in figure 3 was obtained by neglecting the off-diagonal acceptor–donor cross-product term in equation (46) and thus represents the effect of the impurity structure factor by itself: a drastic increase of the charge relaxation rate. Once the acceptor–donor cross-product term is taken into account, the ionic screening of disorder potential

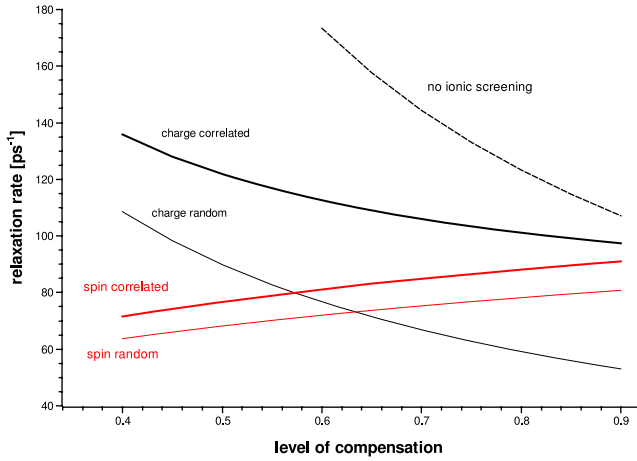


Figure 3. Charge and spin relaxation rates for randomly distributed and correlated impurities in $\text{Ga}_{0.95}\text{Mn}_{0.05}\text{As}$ as a function of the level of compensation (number of holes per Mn_{Ga}). See the text for details.

results in a significant decrease of the charge relaxation rate. As expected, the most significant effect of ionic screening takes place for heavily compensated systems. Nevertheless, the combined effect of ionic screening and impurity structure factor results in a net increase of the charge relaxation rate for correlated impurities for the whole range of compensations. The increase is significant (up to 100%) and is sensitive to cluster configuration. The spin relaxation rates were calculated for interacting localized spins (with $T_c = 150$ K) at room temperature. The positional correlation of localized spins also results in an increase of the spin relaxation rate. This increase, however, is smaller than for charge scattering.

5. Electron–electron interaction and collective modes

Most previous studies of (magneto)transport in DMS include electronic many-body effects only in the form of static Coulomb screening [14, 15, 40]. However, this simplification ignores the role of dynamical many-body effects such as the coupling to collective modes. A major advantage of our formalism is that it allows us to consider both disorder and electron–electron interaction on an equal footing. All carrier many-body effects in equation (27) including screening, correlations and collective excitations are absorbed in the set of density and spin-density response functions. In sections 3 and 4, the effects of electron–electron interaction were reduced to simple static screening of the disorder potential (32). In principle, however, all these effects can be accounted for exactly by means of time-dependent density-functional theory [24]. In the original work by Gross and Kohn [41], the interacting density–density response function of a homogeneous system is shown to be representable as

$$\chi^{-1}(\mathbf{q}, \omega) = \chi_0^{-1}(\mathbf{q}, \omega) - v(q) - f_{xc}(\mathbf{q}, \omega), \quad (55)$$

where $v(q)$ is the Coulomb interaction and f_{xc} is the exchange–correlation kernel.

Coupling to the charge plasmon mode already occurs at the level of dynamic RPA, corresponding to the first two terms

on the right-hand side of equation (55). For multicomponent response functions the corresponding equation has the matrix form

$$\underline{\chi}_{\text{RPA}}^{-1}(\mathbf{q}, \omega) = \underline{\chi}_0^{-1}(\mathbf{q}, \omega) - \underline{v}, \quad (56)$$

where $\underline{\chi}$ are the matrices of charge- and spin-density response functions and \underline{v} is the interaction matrix. Its components v_{ij} describe the interaction between i th and j th components of the multicomponent vector of observables $\hat{\rho}$. Since at the RPA level only the Hartree part of the electron–electron interaction is taken into account, the matrix \underline{v} has the simple form

$$\underline{v} = v(q) \begin{pmatrix} 1 & 0 & 0 & 0 \\ 0 & 0 & 0 & 0 \\ 0 & 0 & 0 & 0 \\ 0 & 0 & 0 & 0 \end{pmatrix}, \quad (57)$$

the only nonvanishing element being the Coulomb interaction between the charges.

The matrix of noninteracting response functions has the form

$$\underline{\chi}_0 = \begin{pmatrix} \chi_{nn}^0 & \chi_{ns^z}^0 & 0 & 0 \\ \chi_{ns^z}^0 & \chi_{nn}^0 & 0 & 0 \\ 0 & 0 & 0 & \chi_{s^+s^-}^0 \\ 0 & 0 & \chi_{s^-s^+}^0 & 0 \end{pmatrix}, \quad (58)$$

with components defined in equation (36), and we have used $\chi_{s^z s^z}^0 = \chi_{nn}^0$. Equation (56) then yields

$$\underline{\chi}_{\text{RPA}} = \begin{pmatrix} \frac{\chi_{nn}^0}{\epsilon_{\text{RPA}}} & \frac{\chi_{ns^z}^0}{\epsilon_{\text{RPA}}} & 0 & 0 \\ \frac{\chi_{ns^z}^0}{\epsilon_{\text{RPA}}} & \frac{\chi_{nn}^0 - v(q)\Lambda}{\epsilon_{\text{RPA}}} & 0 & 0 \\ 0 & 0 & 0 & \chi_{s^+s^-}^0 \\ 0 & 0 & \chi_{s^-s^+}^0 & 0 \end{pmatrix}, \quad (59)$$

where

$$\epsilon_{\text{RPA}} = 1 - v(q)\chi_{nn}^0(q, \omega) \quad (60)$$

and

$$\Lambda = (\chi_{nn}^0)^2 - (\chi_{ns^z}^0)^2 = 4\chi_{\uparrow}^0\chi_{\downarrow}^0. \quad (61)$$

The appearance of collective excitations is immediately seen in the charge response function in equation (59). Some technical details of dealing with the plasmon singularity are presented in appendix E. Let us make here a brief remark about the origin of collective excitations. In isotropic systems the longitudinal plasmons cannot be directly excited by a transversal electromagnetic field. Plasmon excitations here are coupled to the Coulomb impurity potential and are a direct consequence of the disorder in the system.

As seen from equation (59), the random phase approximation does not affect the spin channel. To capture collective spin modes one has to go beyond RPA and include exchange and correlation contributions in equation (55). The generalized charge–spin exchange–correlation kernels are arranged as a symmetrical 4×4 matrix \underline{f} . If the z axis is oriented along the average spin, then the ground-state

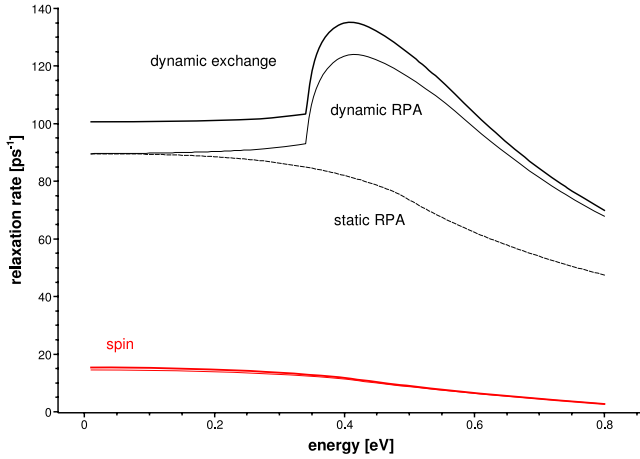


Figure 4. Frequency dependence of the charge and spin relaxation rates for ferromagnetic $\text{Ga}_{0.95}\text{Mn}_{0.05}\text{As}$ with electron–electron interaction taken into account within static RPA, dynamic RPA and dynamic exchange models.

transversal spin densities ρ_+ and ρ_- vanish and the matrix $\underline{\underline{f}}$ becomes block-diagonal:

$$\underline{\underline{f}} = \begin{pmatrix} f_{00} & f_{0z} & 0 & 0 \\ f_{0z} & f_{zz} & 0 & 0 \\ 0 & 0 & 0 & f_{+-} \\ 0 & 0 & f_{+-} & 0 \end{pmatrix}. \quad (62)$$

The expressions for the components of the exchange-correlation matrix for a partially spin-polarized electron gas in the local spin-density approximation were obtained in [42]. For simplicity, we here use only the exchange part of f_{xc} . After matrix inversion we obtain the tensor of response functions featuring local field factors (LFF):

$$\underline{\underline{\chi}}_{\text{LFF}} = \begin{pmatrix} \frac{\chi_{nn}^0 - f_{zz}\Lambda}{\epsilon_{\text{LFF}}} & \frac{\chi_{ns^z}^0 + f_{0z}\Lambda}{\epsilon_{\text{LFF}}} & 0 & 0 \\ \frac{\chi_{ns^z}^0 + f_{0z}\Lambda}{\epsilon_{\text{LFF}}} & \frac{\chi_{nn}^0 - (v(q) + f_{00})\Lambda}{\epsilon_{\text{LFF}}} & 0 & 0 \\ 0 & 0 & 0 & \frac{\chi_{s^+s^-}^0}{1 - f_{+-}\chi_{s^+s^-}^0} \\ 0 & 0 & \frac{\chi_{s^-s^+}^0}{1 - f_{+-}\chi_{s^-s^+}^0} & 0 \end{pmatrix}, \quad (63)$$

where

$$\epsilon_{\text{LFF}} = 1 - (v(q) + f_{00} + f_{zz})\chi_{nn}^0(q, \omega) - 2f_{0z}\chi_{ns^z}^0(q, \omega) + (f_{zz}(v(q) + f_{00}) - f_{0z}^2)\Lambda. \quad (64)$$

Results for the frequency dependence of charge and spin relaxation rates for ferromagnetic $\text{Ga}_{0.95}\text{Mn}_{0.05}\text{As}$ are presented in figure 4. Coupling to the plasmon modes that appear in dynamic RPA results in a strong enhancement of the charge relaxation rate since it provides an efficient channel to absorb the momentum from impurity scattering. Inclusion of the exchange interaction term in the local field factors approximation further slightly increases the charge relaxation rate.

The form of the energy denominators in the transverse spin response functions in equation (63) suggests the theoretical possibility of collective spin excitations. However, our single-band model does not produce any spin collective mode. In fact, the change from the spin relaxation rates calculated for noninteracting electron gas is barely noticeable. A different scenario might take place in a more realistic model with multiple valence bands [32]. In this model the long-wavelength spectrum of single-particle excitations is dominated by vertical inter-valence band spin transitions, which suggests the possibility that collective inter-valence band modes may play a role. This is currently work in progress [32].

6. Conclusions

We have presented a general theory of electron transport in spin and charge disordered media, aimed at describing transport and optical properties of DMSs like $\text{Ga}_{1-x}\text{Mn}_x\text{As}$ with emphasis given to disorder. The approach is based on the equation of motion for the current response function and treats disorder effects and electron–electron interaction on an equal footing. Within this paper, calculations were performed in the weak disorder limit and using the simple model of a single parabolic valence band.

We have shown that, for typical material parameters, the Coulomb scattering off charged defects and exchange scattering off fluctuations of localized spin moments are of the same order of magnitude and should, therefore, be considered simultaneously. We have argued that the suppression of the localized spin fluctuations in the ferromagnetic phase causes a drastic reduction of the spin scattering. This should contribute to the experimentally observed drop in resistivity below critical temperature [27]. In systems with positional correlation of the defects, the combined effect of ionic screening and impurity structure factor results in a net increase of the relaxation rate.

A major advantage of our approach is the possibility to treat dynamical many-body effects in principle exactly using the time-dependent density-functional formalism. We have shown that the coupling to the charge plasmon mode substantially modifies the frequency dependence of the relaxation rate, which may be important for an accurate description of the infrared absorption spectrum of DMSs. We would like to point out that the coupling to collective electronic modes cannot be easily described with the basic textbook approach for impurity scattering using the relaxation time approximation [43], where scattering rates are directly calculated with Fermi’s Golden Rule.

While the single-band approximation used in this paper has obvious limitations, it has the advantage that the derivations are more transparent than in a multiband case, while the essential physics (for instance, the effects of impurity correlations, or of collective electronic modes) are captured at least qualitatively correctly. More comprehensive calculations based on an eight-band $\mathbf{k}\cdot\mathbf{p}$ model to describe the host material band structure are currently in progress.

Acknowledgment

This work was supported by DOE grant no. DE-FG02-05ER46213.

Appendix A. Spin- and charge-density response functions for a noninteracting spin-polarized electron gas

We write the electronic part of the clean system Hamiltonian (9) in the form

$$\hat{H}_e = \sum_{\mathbf{k}, \sigma} \varepsilon(\mathbf{k}, \sigma) \hat{a}_{\mathbf{k}\sigma}^\dagger \hat{a}_{\mathbf{k}\sigma}, \quad (\text{A.1})$$

which is diagonal in a plane wave basis and accounts for possible spin splitting, e.g. due to the mean field part of the p-d exchange interaction. Equation (28) can be directly evaluated, resulting in

$$\chi_{\rho^\mu \rho^\nu}(\mathbf{q}, \omega) = \frac{1}{V} \sum_{\mathbf{k}, \sigma, \sigma'} \frac{f_{\mathbf{k}-\mathbf{q}, \sigma} - f_{\mathbf{k}, \sigma'}}{\hbar\omega + \varepsilon_{\mathbf{k}-\mathbf{q}, \sigma} - \varepsilon_{\mathbf{k}, \sigma'} + i\eta} (\hat{\sigma}^\mu)_{\sigma\sigma'} (\hat{\sigma}^\nu)_{\sigma'\sigma}, \quad (\text{A.2})$$

where $\sigma, \sigma' = \uparrow, \downarrow$ and $f_{\mathbf{k}, \sigma}$ are the spin-dependent Fermi distribution. Direct analysis of equation (A.2) shows that the only nonvanishing elements of the tensor $\underline{\chi}$ are

$$\chi_{nn} = \chi_{s^z s^z} = \chi_0^\uparrow + \chi_0^\downarrow, \quad \chi_{s^z n} = \chi_{ns^z} = \chi_0^\uparrow - \chi_0^\downarrow,$$

$$\chi_{s^+ s^-}(\mathbf{q}, \omega) = \chi_{s^- s^+}^*(-\mathbf{q}, -\omega),$$

where

$$\chi_0^\sigma(\mathbf{q}, \omega) = \frac{1}{V} \sum_{\mathbf{k}} \frac{f_{\mathbf{k}-\mathbf{q}, \sigma} - f_{\mathbf{k}, \sigma}}{\hbar\omega + \varepsilon_{\mathbf{k}-\mathbf{q}, \sigma} - \varepsilon_{\mathbf{k}, \sigma} + i\eta}$$

is the well-known spin-resolved Lindhard function and

$$\chi_{s^+ s^-}(\mathbf{q}, \omega) = \frac{1}{V} \sum_{\mathbf{k}} \frac{f_{\mathbf{k}-\mathbf{q}, \uparrow} - f_{\mathbf{k}, \downarrow}}{\hbar\omega + \varepsilon_{\mathbf{k}-\mathbf{q}, \uparrow} - \varepsilon_{\mathbf{k}, \downarrow} + i\eta}$$

is the off-diagonal spin response function. Assuming a momentum-independent spin splitting

$$\Delta = \varepsilon_{\mathbf{k}\uparrow} - \varepsilon_{\mathbf{k}\downarrow}, \quad (\text{A.3})$$

these response functions can be expressed through a single quantity

$$A_\sigma(\mathbf{q}, \hbar\omega) = \frac{1}{V} \sum_{\mathbf{k}} \frac{f_{\mathbf{k}, \sigma}}{\hbar\omega + \varepsilon_{\mathbf{k}-\mathbf{q}} - \varepsilon_{\mathbf{k}} + i\eta} \quad (\text{A.4})$$

in the following way:

$$\chi_0^\sigma(\mathbf{q}, \omega) = -A_\sigma^*(-\mathbf{q}, -\hbar\omega) - A_\sigma(\mathbf{q}, \hbar\omega), \quad (\text{A.5})$$

and

$$\chi_{s^+ s^-}(\mathbf{q}, \omega) = -A_\uparrow^*(-\mathbf{q}, -\hbar\omega - \Delta) - A_\downarrow(\mathbf{q}, \hbar\omega + \Delta). \quad (\text{A.6})$$

Given the band structure dispersion, the real and imaginary parts of A_σ can be directly evaluated. For a simple parabolic dispersion $E_q = \frac{\hbar^2 q^2}{2m}$, straightforward calculation gives

$$\text{Re}[A_\sigma(\mathbf{q}, \omega)] = \frac{m}{4\pi^2 \hbar^2 q} \int_0^\infty k f_{k\sigma} \times \log \left| \frac{q^2 + 2kq + 2m\omega/\hbar}{q^2 - 2kq + 2m\omega/\hbar} \right| dk$$

and

$$\text{Im}[A_\sigma(\mathbf{q}, \omega)] = -\frac{1}{8\pi} \frac{q}{E_q} \int_{k_{\min}}^\infty k f_{k\sigma} dk,$$

with

$$k_{\min} = \frac{q}{2} \left| 1 + \frac{\hbar\omega}{E_q} \right|.$$

Both real and imaginary parts depend only on the magnitude of the wavevector \mathbf{q} , as they should in an isotropic system.

At low carrier temperature, when the distribution functions $f_{k\sigma}$ can be approximated as step functions, the above expressions are easily integrated to

$$\text{Re}[A_\sigma(q, \omega)] = \frac{1}{8\pi^2} \frac{q (k_F^\sigma)^2}{E_q} \left(\alpha + \frac{1 - \alpha^2}{2} \log \left| \frac{\alpha + 1}{\alpha - 1} \right| \right) \quad (\text{A.7})$$

with

$$\alpha = \frac{q}{2k_F^\sigma} \left(1 + \frac{\hbar\omega}{E_q} \right),$$

and

$$\text{Im}[A_\sigma(q, \omega)] = \begin{cases} -\frac{1}{16\pi} \frac{q ((k_F^\sigma)^2 - k_{\min}^2)}{E_q}, & k_F^\sigma > k_{\min} \\ 0, & k_F^\sigma < k_{\min}. \end{cases} \quad (\text{A.8})$$

Appendix B. Discussion of χ_A in equation (27)

χ_A in equation (27) is the sum of two terms, $\chi_A = \chi_A^{(3)} + \chi_A^{(4)}$, where

$$\chi_A^{(3)} = \frac{V^2}{m^2 \omega^2} \sum_{\mathbf{k}, \mathbf{k}'} k_\alpha k'_\beta \sum_{\mu\nu} \left\langle \left[\hat{U}_\mu(\mathbf{k}), \hat{U}_\nu(\mathbf{k}') \right] \right\rangle_{H_m} \times \frac{iV}{\hbar} \int_0^\infty \langle \hat{\rho}_\nu(-\mathbf{q} - \mathbf{k}') \hat{\rho}_\mu(\mathbf{q} - \mathbf{k}, \tau) \rangle_{H_e + H_I} e^{i(\omega + i\eta)\tau} d\tau,$$

and

$$\chi_A^{(4)} = \frac{V^2}{m^2 \omega^2} \sum_{\mathbf{k}, \mathbf{k}'} (k_\alpha + q_\alpha) k_\beta \sum_{\mu\nu} \left\langle \left[\hat{U}_\mu(\mathbf{k}), \hat{U}_\nu(\mathbf{k}') \right] \right\rangle_{H_m} \times \frac{iV}{\hbar} \int_0^\infty \langle \hat{\rho}_\nu(-\mathbf{k}') \hat{\rho}_\mu(-\mathbf{k}, \tau) \rangle_{H_e} e^{-\eta\tau} d\tau.$$

In general, these terms arise from the noncommutativity of the components of the spin-dependent disorder potential (31).

It is found that in our model the corresponding commutators either vanish or are linear in the localized spin operators. We immediately conclude that in paramagnetic systems both additional terms would vanish after thermodynamical averaging.

If there is a finite magnetization of the localized spin subsystem, then direct calculation using equation (31) and the commutation relations $[\hat{S}^+, \hat{S}^-] = 2\hat{S}_z$ allows us to rewrite

$$\begin{aligned}\chi_A^{(3)} &= \frac{V^2}{m^2\omega^2} \frac{J^2 \langle S_z \rangle}{2V} \sum_{\mathbf{k}, \mathbf{k}'} k_\alpha k'_\beta n_I(\mathbf{k} + \mathbf{k}') \frac{iV}{\hbar} \\ &\times \int_0^\infty \mathcal{F}(\mathbf{q}, \mathbf{k}, \mathbf{k}', \tau) e^{i(\omega+i\eta)\tau} d\tau, \\ \chi_A^{(4)} &= \frac{V^2}{m^2\omega^2} \frac{J^2 \langle S_z \rangle}{2V} \sum_{\mathbf{k}, \mathbf{k}'} (k_\alpha + q_\alpha) k_\beta n_I(\mathbf{k} + \mathbf{k}') \frac{iV}{\hbar} \\ &\times \int_0^\infty \mathcal{F}^c(\mathbf{0}, \mathbf{k}, \mathbf{k}', \tau) e^{-\eta\tau} d\tau,\end{aligned}$$

where $n_I(\mathbf{k})$ is the Fourier transform of the density of impurities,

$$\begin{aligned}\mathcal{F}(\mathbf{q}, \mathbf{k}, \mathbf{k}', \tau) &= \langle \hat{\rho}^+(-\mathbf{q} - \mathbf{k}') \hat{\rho}^-(\mathbf{q} - \mathbf{k}, \tau) \rangle_{H_c + H_d} \\ &- \langle \hat{\rho}^-(-\mathbf{q} - \mathbf{k}') \hat{\rho}^+(\mathbf{q} - \mathbf{k}, \tau) \rangle_{H_c + H_d},\end{aligned}$$

and \mathcal{F}^c means that averaging is performed over the clean system Hamiltonian \hat{H}_c .

In general, $\chi_A^{(3)}$ is a full system quantity and, as such, should be evaluated iteratively along with other full system response functions on the right-hand side of equation (27). As mentioned above, however, for weak disorder we can substitute the full system quantities by their clean system counterparts. In that case, one finds

$$\begin{aligned}\mathcal{F}^c(\mathbf{q}, \mathbf{k}, \mathbf{k}', \tau) &= \delta_{\mathbf{k}, -\mathbf{k}'} \frac{1}{V^2} \\ &\times \sum_{\tilde{\mathbf{k}}} \left\{ e^{\frac{i}{\hbar}(\varepsilon_{\tilde{\mathbf{k}}, \downarrow} - \varepsilon_{\tilde{\mathbf{k}}, \uparrow})\tau} f_{\tilde{\mathbf{k}}-\tilde{\mathbf{q}}, \uparrow} (1 - f_{\tilde{\mathbf{k}}, \downarrow}) \right. \\ &\left. - e^{\frac{i}{\hbar}(\varepsilon_{\tilde{\mathbf{k}}, \uparrow} - \varepsilon_{\tilde{\mathbf{k}}, \downarrow})\tau} f_{\tilde{\mathbf{k}}-\tilde{\mathbf{q}}, \downarrow} (1 - f_{\tilde{\mathbf{k}}, \uparrow}) \right\},\end{aligned}$$

with $\tilde{\mathbf{q}} = \mathbf{k} - \mathbf{q}$. Note that \mathcal{F} vanishes if there is no spin splitting in the clean system, i.e. if $\varepsilon_{\mathbf{k}, \uparrow} = \varepsilon_{\mathbf{k}, \downarrow}$ and, consequently, $f_{\mathbf{k}, \uparrow} = f_{\mathbf{k}, \downarrow}$. Therefore, the additional term χ_A vanishes in the clean system approximation if there is no spin splitting in the electron liquid.

After carrying out the integrations we obtain

$$\begin{aligned}\chi^A &= \frac{n_i V J^2}{2m^2\omega^2} \langle S_z \rangle \sum_{\mathbf{k}} k_\alpha k_\beta [A_\uparrow(\mathbf{q} - \mathbf{k}, \hbar\omega - \Delta) \\ &- A_\uparrow(k, -\Delta) - A_\downarrow(\mathbf{q} - \mathbf{k}, \hbar\omega + \Delta) \\ &+ A_\downarrow(k, \Delta)] + \chi_B^{(3)} + \chi_B^{(4)},\end{aligned}\quad (\text{B.1})$$

where n_i is the impurity concentration, the quantities A_σ are given by equations (A.7) and (A.8), and

$$\begin{aligned}\chi_B^{(3)} &= \frac{n_i V J^2}{2m^2\omega^2} \langle S_z \rangle \sum_{\mathbf{k}} k_\alpha k_\beta \frac{1}{V} \sum_{\tilde{\mathbf{k}}} \left(\frac{f_{\tilde{\mathbf{k}}-\tilde{\mathbf{q}}, \downarrow} f_{\tilde{\mathbf{k}}, \uparrow}}{\varepsilon_{\tilde{\mathbf{k}}, \uparrow} - \varepsilon_{\tilde{\mathbf{k}}-\tilde{\mathbf{q}}, \downarrow} + \hbar\omega + i\eta} \right. \\ &\left. - \frac{f_{\tilde{\mathbf{k}}-\tilde{\mathbf{q}}, \uparrow} f_{\tilde{\mathbf{k}}, \downarrow}}{\varepsilon_{\tilde{\mathbf{k}}, \downarrow} - \varepsilon_{\tilde{\mathbf{k}}-\tilde{\mathbf{q}}, \uparrow} + \hbar\omega + i\eta} \right), \\ \chi_B^{(4)} &= -\frac{n_i V J^2}{2m^2\omega^2} \langle S_z \rangle \sum_{\mathbf{k}} (k_\alpha + q_\alpha) k_\beta \frac{1}{V} \sum_{\tilde{\mathbf{k}}} \left(\frac{f_{\tilde{\mathbf{k}}-\mathbf{k}, \downarrow} f_{\tilde{\mathbf{k}}, \uparrow}}{\varepsilon_{\tilde{\mathbf{k}}, \uparrow} - \varepsilon_{\tilde{\mathbf{k}}-\mathbf{k}, \downarrow}} \right. \\ &\left. - \frac{f_{\tilde{\mathbf{k}}-\mathbf{k}, \uparrow} f_{\tilde{\mathbf{k}}, \downarrow}}{\varepsilon_{\tilde{\mathbf{k}}, \downarrow} - \varepsilon_{\tilde{\mathbf{k}}-\mathbf{k}, \uparrow}} \right).\end{aligned}$$

$\chi_B^{(3)}$ and $\chi_B^{(4)}$ are proportional to products of two distribution functions (for spin up and spin down), which means that these terms would vanish not only in the paramagnetic case, but at full spin polarization of the electron liquid as well. They would be nonzero only in the case of partial spin polarization. Even then, the product of two distribution functions with different arguments will be substantially smaller after integration over $\tilde{\mathbf{k}}$ as compared to terms containing only a single distribution function. Therefore, we neglect $\chi_B^{(3)}$ and $\chi_B^{(4)}$, and we will take expression (38) for χ_A in equation (27).

Appendix C. Momentum-dependent impurity structure factor

Let us begin by considering the diagonal term in equation (47) with $i = i'$ (to simplify the notation we will drop all super- and subscript i while dealing with the diagonal term):

$$\begin{aligned}\langle \hat{U}_n(\mathbf{k}) \hat{U}_n(-\mathbf{k}) \rangle_{H_m} &= |U_n(\mathbf{k})|^2 \left(\frac{n_i}{V} + \frac{2}{V^2} \sum_{j>j'} \cos(\mathbf{k} \cdot \mathbf{R}_{jj'}) \right) \\ &= |U_n(\mathbf{k})|^2 \frac{n_i}{V} S(\mathbf{k}),\end{aligned}\quad (\text{C.1})$$

where the impurity structure factor $S(\mathbf{k})$ is given by

$$\begin{aligned}S(\mathbf{k}) &= 1 + \frac{2}{N_i} \sum_{j>j'} \cos(\mathbf{k} \cdot \mathbf{R}_{jj'}) \\ &\approx 1 + \frac{2}{N_i} \sum_{i=1}^{\tilde{N}} P(\mathbf{R}) \cos(\mathbf{k} \cdot \mathbf{R}),\end{aligned}\quad (\text{C.2})$$

i.e. we substitute the sum over the real positions of magnetic ions by the sum of

$$\tilde{N} = \binom{2}{N_i} = \frac{N_i!}{2!(N_i - 2)!} = \frac{N_i(N_i - 1)}{2} \approx \frac{N_i^2}{2}$$

random quantities $\cos(\mathbf{k} \cdot \mathbf{R})$ distributed with probability $P(\mathbf{R})$. The structure factor is now a sum of \tilde{N} random quantities, and for $\tilde{N} \rightarrow \infty$ we can substitute the random quantity $S(\mathbf{k})$ by its expectation value

$$S(\mathbf{k}) \approx \langle S(\mathbf{k}) \rangle = 1 + N_i \langle \cos(\mathbf{k} \cdot \mathbf{R}) \rangle.\quad (\text{C.3})$$

We have

$$\langle \cos(\mathbf{k} \cdot \mathbf{R}) \rangle = \sum_{\mathbf{R}} P(\mathbf{R}) \cos(\mathbf{k} \cdot \mathbf{R}),\quad (\text{C.4})$$

where the summation is performed over all possible distances \mathbf{R} . The pair distribution function $P(\mathbf{R})$ is the probability that the given pair of defects is separated by a distance \mathbf{R} and is given by the general expression

$$P(\mathbf{R}) = \sum_{\mathbf{R}_1} P_1(\mathbf{R}_1) P_{2/1}(\mathbf{R}, \mathbf{R}_1),\quad (\text{C.5})$$

where $P_1(\mathbf{R}_1)$ is the probability for the first defect of the pair to sit at \mathbf{R}_1 and $P_{2/1}(\mathbf{R}, \mathbf{R}_1)$ is the *conditional* probability for the second defect to sit at $\mathbf{R}_2 = \mathbf{R}_1 + \mathbf{R}$, provided that the first defect is at \mathbf{R}_1 . The general expression (C.5) allows us to describe nonhomogeneous distributions of impurities

like digital alloy structures as well as macroscopically homogeneous systems with correlated impurities.

In macroscopically homogeneous cases the probability distribution $P_1(\mathbf{R}_i)$ is uniform, and from the normalization condition $\sum_{i=1}^{N_0} P_1(\mathbf{R}_i) = 1$ we have $P_1(\mathbf{R}_i) = 1/N_0$, where N_0 is the number of elementary cells. The conditional probability for macroscopically homogeneous systems should depend only on the distance from the first defect \mathbf{R} , but not from its position \mathbf{R}_1 : $P_{2/1} \equiv P_{2/1}(\mathbf{R})$. Consequently, equation (C.5) becomes

$$P(\mathbf{R}) = \sum_{\mathbf{R}_1} \frac{1}{N_0} P_{2/1}(\mathbf{R}) = N_0 \frac{1}{N_0} P_{2/1}(\mathbf{R}) = P_{2/1}(\mathbf{R}), \quad (\text{C.6})$$

and the pair distribution function equals the conditional probability $P_{2/1}(\mathbf{R})$.

For uncorrelated impurities all distances \mathbf{R} are equally probable and the conditional probability is uniform: $P_{2/1}^{\text{un}}(\mathbf{R}) = 1/N_0$. Therefore, for randomly distributed defects the structure factor (C.3) is

$$S_r(\mathbf{k}) = 1 + \frac{N_i}{N_0} \sum_{i=1}^{N_0} \cos(\mathbf{k} \cdot \mathbf{R}_i). \quad (\text{C.7})$$

By introducing a convergence factor it can be shown that the sum on the right-hand side of equation (C.7) vanishes for nonzero k :

$$\begin{aligned} \sum_{i=1}^{N_0} \cos(\mathbf{k} \cdot \mathbf{R}_i) &\approx \lim_{\eta \rightarrow 0^+} \sum_{i=1}^{N_0} \cos(\mathbf{k} \cdot \mathbf{R}_i) e^{-\eta R} \\ &\approx \lim_{\eta \rightarrow 0^+} \frac{N_0}{V} \int_V \cos(\mathbf{k} \cdot \mathbf{R}) e^{-\eta R} d\mathbf{R} \\ &= \lim_{\eta \rightarrow 0^+} \frac{4\pi N_0}{Vk} \frac{2\eta k}{(\eta^2 + k^2)^2} = 0. \end{aligned}$$

Therefore, for random impurity distributions the structure factor is $S_r(\mathbf{k}) = 1$.

If there are correlations in the impurity positions, then we write

$$P_{2/1}(\mathbf{R}) = P(\mathbf{R}) = \frac{1}{N_0} + \tilde{P}(\mathbf{R}),$$

and thus

$$\langle \cos(\mathbf{k} \cdot \mathbf{R}) \rangle = \sum_{i=1}^{N_0} \tilde{P}(\mathbf{R}_i) \cos(\mathbf{k} \cdot \mathbf{R}_i). \quad (\text{C.8})$$

The function $P(\mathbf{R})$ must satisfy normalization, which implies

$$\sum_{i=1}^{N_0} \tilde{P}(\mathbf{R}_i) = \frac{N_0}{V} \int_V \tilde{P}(\mathbf{R}) d\mathbf{R} = 0.$$

In our calculations we assume \tilde{P} to be a piecewise continuous, spherically symmetrical function of the form

$$\tilde{P}(R) = \begin{cases} \frac{x' - x}{N_i}, & R < R_1, \\ -\frac{x}{2N_i}, & R_1 < R < R_2, \\ 0, & R > R_2. \end{cases} \quad (\text{C.9})$$

The first region describes a cluster of radius R_1 with effective impurity concentration $x' > x$, where $x = N_i/N_0$ is the average impurity concentration in the sample. Then follows a depletion layer up to $R = R_2$ with effective impurity concentration between 0 and x . Our calculations show that the particular choice of impurity concentration within the depletion layer has little effect on the final results, so we fixed it to the value $x/2$. The width of the depletion layer is determined by the condition $R_2 = (\frac{2x'-x}{x})^{1/3} R_1$. Two independent parameters remain to describe the cluster: the cluster radius R_1 and the effective impurity concentration within the cluster x' . By fixing the average number N of impurities within the cluster we can relate them through $\frac{4\pi R_1^3}{3\Omega_0} x' = N$, where Ω_0 is the primitive cell volume. Throughout our calculations we use the average number $N = 10$ of Mn_{Ga} defects within the cluster, which roughly corresponds to the results of the Monte Carlo simulations of [38].

The diagonal term structure factor (C.3) thus has the form

$$S(\mathbf{k}) = 1 + \frac{n_i V}{\Omega_0} \int_V \tilde{P}(\mathbf{R}) \cos(\mathbf{k} \cdot \mathbf{R}) d\mathbf{R}, \quad (\text{C.10})$$

and direct integration gives

$$\begin{aligned} S(k) = 1 + \frac{2\pi x}{k^3 \Omega_0} &\left\{ \left(\frac{2x'}{x} - 1 \right) [\sin(kR_1) - kR_1 \cos(kR_1)] \right. \\ &\left. - [\sin(kR_2) - kR_2 \cos(kR_2)] \right\}. \end{aligned}$$

The off-diagonal cross-products with $i \neq i'$ in equation (47) involve essentially different defects and thus have only the pair term:

$$\left\langle \hat{U}_n^i(\mathbf{k}) \hat{U}_n^{i'}(-\mathbf{k}) \right\rangle_{H_m} = \frac{1}{V^2} U_n^i(\mathbf{k}) U_n^{i'}(-\mathbf{k}) \sum_{j \neq j'} e^{i\mathbf{k} \cdot (\mathbf{R}_{j'}^i - \mathbf{R}_j^{i'})}. \quad (\text{C.11})$$

Again, within the framework of probability theory we assume

$$\begin{aligned} \frac{1}{V^2} \sum_{j \neq j'} e^{i\mathbf{k} \cdot (\mathbf{R}_{j'}^i - \mathbf{R}_j^{i'})} &\approx \frac{N_i N_{i'}}{V^2} \langle e^{i\mathbf{k} \cdot \mathbf{R}_{j'}^{i'}} \rangle \\ &= \frac{n_i n_{i'}}{\Omega_0} \int_V P_{ii'}(R) \cos(\mathbf{k} \cdot \mathbf{R}) d\mathbf{R}. \end{aligned}$$

The pair distribution function is once again written in the form

$$P_{ii'}(\mathbf{R}) = \frac{1}{N_0} + \tilde{P}_{ii'}(\mathbf{R}), \quad (\text{C.12})$$

where $\tilde{P}_{ii'}$ defines the acceptor–donor correlation function. We again use the form (C.9), additionally assuming that the double donor always sits near one of the acceptors, thus forming an interstitial substitutional pair. The off-diagonal cross-product structure factor is then

$$S_{ii'}(\mathbf{k}) = \frac{n_i V}{\Omega_0} \int_V \tilde{P}_{ii'}(\mathbf{R}) \cos(\mathbf{k} \cdot \mathbf{R}) d\mathbf{R}. \quad (\text{C.13})$$

Appendix D. Interacting spins in high-temperature expansion

We need to calculate the two-spin correlation function:

$$\left\langle \hat{S}_j^\mu \hat{S}_{j'}^\nu \right\rangle_{H_m} = \frac{\text{Tr} e^{-\beta \hat{H}_m} \hat{S}_j^\mu \hat{S}_{j'}^\nu}{\text{Tr} e^{-\beta \hat{H}_m}}, \quad (\text{D.1})$$

where $\mu, \nu = x, y, z$ and the spin Hamiltonian is given by equation (51). In the high-temperature (weak interaction) limit $J\beta \rightarrow 0$, we use the following expansion:

$$e^{-\beta \hat{H}_m} \approx 1 - \beta \hat{H}_m + \mathcal{O}((\beta H_m)^2). \quad (\text{D.2})$$

Substitution into equation (D.1) yields

$$\begin{aligned} \left\langle \hat{S}_j^\mu \hat{S}_{j'}^\nu \right\rangle_{H_m} &\approx \text{Tr} \left(-\beta \hat{H}_m \hat{S}_j^\mu \hat{S}_{j'}^\nu \right) \\ &= \frac{\beta}{2} \sum_{i \neq i'} J_{ii'} \sum_{\tau} \text{Tr} \left(\hat{S}_i^\tau \hat{S}_{i'}^\tau \hat{S}_j^\mu \hat{S}_{j'}^\nu \right) \\ &= \beta J_{jj'} \delta_{\mu\nu} \left(\text{Tr} \hat{S}_\mu^2 \right)^2 = \beta J_{jj'} \delta_{\mu\nu} \left(\frac{S(S+1)}{3} \right)^2. \end{aligned}$$

This derivation is valid for temperatures far above T_c and for zero magnetic field.

The Mn–Mn exchange constant $J_{jj'} = J_{jj'}(\mathbf{R}) = J_{jj'}(\mathbf{R}_j - \mathbf{R}_{j'})$ is assumed to be the sum of two spherically symmetric contributions:

$$J_{jj'}(R) = J_F(R) + J_A(R), \quad (\text{D.3})$$

with

$$\begin{aligned} J_F(R) &= \begin{cases} J_F, & R < R_F, \\ 0, & R > R_F, \end{cases} \\ J_A(R) &= \begin{cases} J_A, & R < R_A, \\ 0, & R > R_A, \end{cases} \end{aligned} \quad (\text{D.4})$$

describing carrier-mediated ferromagnetic interaction and short-range superexchange antiferromagnetic interaction. We set $R_F \approx 2/k_F$, which roughly corresponds to the first zero of the exchange interaction constant within RKKY. We express the amplitude of the exchange constant as

$$J_F = \frac{3}{4\pi} \frac{J_0 \Omega_0}{R_F^3 x},$$

where $J_0 = \sum_{\mathbf{R}} J(\mathbf{R})$ is extracted from the mean field expression for T_c [31]:

$$J_0 = \frac{3k_B T_c}{S(S+1)}.$$

Typical values are $R_F \sim 8 \text{ \AA}$, $J_0 \sim 3 \text{ meV}$, and thus $J_F \sim 1.5 \text{ meV}$. For the antiferromagnetic exchange constant we choose R_A to be the radius of the elementary cell and $J_A \sim -4 \text{ meV}$ [39].

Appendix E. Plasmon singularity

Due to the presence of ε_{RPA} in the denominator in equation (59), the integration over momentum in equation (43) acquires a contribution from the plasmon pole. The general procedure to account for this contribution is outlined in the following.

The plasmon dispersion $\Omega_p(k)$ is determined by

$$\varepsilon_{\text{RPA}} = 1 - v(k) \chi_{nn}^0(k, \Omega_p) = 0.$$

Away from the single-particle excitation region, the imaginary part of the noninteracting response function for both spins vanishes: $\text{Im} \chi_{\uparrow}^0 = \text{Im} \chi_{\downarrow}^0 = 0$. First we expand ε_{RPA} around the plasmon frequency up to first order in $\omega - \Omega_p$:

$$\varepsilon_{\text{RPA}} \approx -v(k) \left. \frac{\partial(\text{Re} \chi_{nn}^0)}{\partial \omega} \right|_{\omega=\Omega_p(k)} (\omega - \Omega_p(k) + i\eta). \quad (\text{E.1})$$

The convergence factor $i\eta$ appears because the plasmon pole must be in the lower complex half-plane. In the vicinity of the plasmon pole we have thus

$$\begin{aligned} \varepsilon_{\text{RPA}}^{-1} &\approx -\frac{1}{v(k) \left. \frac{\partial(\text{Re} \chi_{nn}^0)}{\partial \omega} \right|_{\omega=\Omega_p(k)}} \\ &\times \left(\mathcal{P} \frac{1}{\omega - \Omega_p(k)} - i\pi \delta(\omega - \Omega_p(k)) \right), \end{aligned} \quad (\text{E.2})$$

where \mathcal{P} denotes the principal value. The contribution to the imaginary part of the RPA response function is proportional to the δ function:

$$\text{Im} \chi_{nn}^{\text{RPA}}|_{\text{plasmon}} = \frac{\pi}{v(k)^2 \left. \frac{\partial(\text{Re} \chi_{nn}^0)}{\partial \omega} \right|_{\omega=\Omega_p(k)}} \delta(\omega - \Omega_p(k)), \quad (\text{E.3})$$

where we have taken into account that $\text{Re} \chi_{nn}^0(k, \Omega_p(k)) = 1/v(k)$ at the plasmon pole. The next step is to change the argument of the δ function:

$$\begin{aligned} \delta(\omega - \Omega_p(k)) &= \delta \left(\omega - \Omega_p(k_0) - \left. \frac{\partial \Omega_p}{\partial k} \right|_{k=k_0} (k - k_0) \right) \\ &= \frac{1}{\left. \frac{\partial \Omega_p}{\partial k} \right|_{k=k_0}} \delta(k - k_0), \end{aligned} \quad (\text{E.4})$$

where k_0 is the plasmon wavevector. Finally, the plasmon contribution to the imaginary part of the RPA response function is given by

$$\text{Im} \chi_{nn}^{\text{RPA}}|_{\text{plasmon}} = \frac{\pi}{v(k)^2 \left. \frac{\partial(\text{Re} \chi_{nn}^0)}{\partial \omega} \right|_{\omega=\Omega_p(k)} \left. \frac{\partial \Omega_p}{\partial k} \right|_{k=k_0}} \delta(k - k_0). \quad (\text{E.5})$$

Using the results of appendix A we can find the explicit expressions for

$$\frac{\partial(\text{Re} \chi_{nn}^0)}{\partial \omega} = \frac{\partial(\text{Re} \chi_{\uparrow}^0)}{\partial \omega} + \frac{\partial(\text{Re} \chi_{\downarrow}^0)}{\partial \omega},$$

with

$$\begin{aligned} \frac{\partial(\text{Re} \chi_{\sigma}^0)}{\partial \omega} &= \frac{1}{8\pi^2} \frac{\hbar k^2 k_F^{\sigma}}{2E_k^2} \left(\alpha_{\sigma}^+ \log \left(\frac{\alpha_{\sigma}^+ + 1}{\alpha_{\sigma}^+ - 1} \right) \right. \\ &\quad \left. - \alpha_{\sigma}^- \log \left(\frac{\alpha_{\sigma}^- + 1}{\alpha_{\sigma}^- - 1} \right) \right) \end{aligned}$$

and

$$\alpha_{\sigma}^{\pm} = \frac{k}{2k_{\text{F}}^{\sigma}} \left(1 \pm \frac{\hbar\omega}{E_k} \right).$$

For small k we can expand

$$\text{Re } \chi_{\sigma}^0(q, \omega) \approx \frac{n_{\sigma} k^2}{m\omega^2} \left(1 + \frac{6 E_{\text{F}}^{\sigma} k^2}{5 m\omega^2} \right),$$

and the plasmon dispersion is

$$\Omega_{\text{p}}(q) = \frac{1}{\sqrt{2}} \left(\omega_{\text{p}}^2 + \sqrt{\omega_{\text{p}}^4 + \frac{24\omega_{\text{p}}^2 k^2}{5m} \frac{n_{\uparrow} E_{\text{F}}^{\uparrow} + n_{\downarrow} E_{\text{F}}^{\downarrow}}{n_{\uparrow} + n_{\downarrow}}} \right)^{1/2}$$

$$\approx \omega_{\text{p}} + \frac{3k^2}{5\omega_{\text{p}} m} \frac{n_{\uparrow} E_{\text{F}}^{\uparrow} + n_{\downarrow} E_{\text{F}}^{\downarrow}}{n_{\uparrow} + n_{\downarrow}},$$

where

$$\omega_{\text{p}}^2 = \frac{4\pi(n_{\uparrow} + n_{\downarrow})e^2}{m}.$$

References

- [1] Prinz G A 1998 *Science* **282** 1660
- [2] Ohno H 1998 *Science* **281** 951
- [3] Edmonds K W, Bogusławski P, Wang K Y, Campion R P, Novikov S N, Farley N R S, Gallagher B L, Foxon C T, Sawicki M, Dietl T, Buongiorno Nardelli M and Bernholc J 2004 *Phys. Rev. Lett.* **92** 037201
- [4] Sinova J, Jungwirth T and Cerne J 2004 *Int. J. Mod. Phys. B* **18** 1083
- [5] Jungwirth T, Sinova J, Mašek J, Kučera J and MacDonald A H 2006 *Rev. Mod. Phys.* **78** 809
- [6] Burch K S, Shrekenhamer D B, Singley E J, Stephens J, Sheu B L, Kawakami R K, Schiffer P, Samarth N, Awschalom D D and Basov D N 2006 *Phys. Rev. Lett.* **97** 087208
- [7] Rokhinson L P, Lyanda-Geller Y, Ge Z, Shen S, Liu X, Dobrowolska M and Furdyna J K 2007 *Phys. Rev. B* **76** 161201
- [8] Jungwirth T, Sinova J, MacDonald A H, Gallagher B L, Novák V, Edmonds K W, Rushforth A W, Campion R P, Foxon C T, Eaves L, Olejník E, Mašek J, Eric Yang S-R, Wunderlich J, Gould C, Molenkamp L W, Dietl T and Ohno H 2007 *Phys. Rev. B* **76** 125206
- [9] Mahadevan P, Zunger A and Sarma D D 2004 *Phys. Rev. Lett.* **93** 177201
- [10] Sandratskii L M, Bruno P and Kudrnovský J 2004 *Phys. Rev. B* **69** 195203
- [11] Berciu M and Bhatt R N 2001 *Phys. Rev. Lett.* **87** 107203
- [12] Dietl T, Ohno H and Matsukura F 2001 *Phys. Rev. B* **63** 195205
- [13] Yildirim Y, Alvarez G, Moreo A and Dalgotto E 2007 *Phys. Rev. Lett.* **99** 057207
- [14] Sinova J, Jungwirth T, Eric Yang S-R, Kučera J and MacDonald A H 2002 *Phys. Rev. B* **66** 041202(R)
- [15] Jungwirth T, Abolfath M, Sinova J, Kučera J and MacDonald A H 2002 *Appl. Phys. Lett.* **81** 4029
- [16] Shimizu H, Hayashi T, Nishinaga T and Tanaka M 1999 *Appl. Phys. Lett.* **74** 398
- [17] Hayashi T, Hashimoto Y, Katsumoto S and Iye Y 2001 *Appl. Phys. Lett.* **78** 1691
- [18] Potashnik S J, Ku K C, Chun S H, Berry J J, Samarth N and Schiffer P 2001 *Appl. Phys. Lett.* **79** 1495
- [19] Yu K M, Walukiewicz W, Wojtowicz T, Kuryliszyn I, Liu X, Sasaki Y and Furdyna J K 2002 *Phys. Rev. B* **65** 201303(R)
- [20] Timm C 2003 *J. Phys.: Condens. Matter* **15** R1865
- [21] Götze W 1981 *Phil. Mag.* **B 43** 219
- [22] Belitz D and Das Sarma S 1986 *Phys. Rev. B* **34** 8264
- [23] Ullrich C A and Vignale G 2002 *Phys. Rev. B* **65** 245102
Ullrich C A and Vignale G 2004 *Phys. Rev. B* **70** 239903 (erratum)
- [24] Marques M A L, Ullrich C A, Nogueira F, Rubio A, Burke K and Gross E K U (ed) 2006 *Time-Dependent Density Functional Theory (Springer Lecture Notes in Physics vol 706)* (Berlin: Springer)
- [25] Kyrychenko F V and Ullrich C A 2007 *Phys. Rev. B* **75** 045205
- [26] Gold A and Götze W 1986 *Phys. Rev. B* **33** 2495
- [27] Omiya T, Matsukura F, Dietl T, Ohno Y, Sakon T, Motokawa M and Ohno H 2000 *Physica E* **7** 976
- [28] See, e.g. Awschalom D D, Loss D and Samarth N (ed) 2002 *Semiconductor Spintronics and Quantum Computation* (Berlin: Springer)
- [29] Lopez-Sancho M P and Brey L 2003 *Phys. Rev. B* **68** 113201
- [30] Mahan G D 2000 *Many-Particle Physics* 3rd edn (New York: Kluwer-Academic)
- [31] Ashcroft N W and Mermin N D 1976 *Solid State Physics* (New York: Saunders)
- [32] Kyrychenko F V and Ullrich C A 2009 unpublished
- [33] Shioda R, Ando K, Hayashi T and Tanaka M 1998 *Phys. Rev. B* **58** 1100
- [34] Soo Y L, Kioseoglou G, Kim S, Chen X, Luo H, Kao Y H, Lin H-J, Hsieh H H, Hou T Y, Chen C T, Sasaki Y, Liu X and Furdyna J K 2003 *Phys. Rev. B* **67** 214401
- [35] Soo Y L, Kim S, Kao Y H, Blattner A J, Wessels B W, Khalid S, Sanchez-Hanke C and Kao C-C 2004 *Appl. Phys. Lett.* **84** 481
- [36] Bouzerar G, Ziman T and Kudrnovsky J 2004 *Appl. Phys. Lett.* **85** 4941
- [37] van Schilfgaarde M and Mryasov O N 2001 *Phys. Rev. B* **63** 233205
- [38] Timm C, Schäfer F and von Oppen F 2002 *Phys. Rev. Lett.* **89** 137201
- [39] Mašek J and Máca F 2003 *Phys. Rev. B* **69** 165212
- [40] Jungwirth T, Niu Q and MacDonald A H 2002 *Phys. Rev. Lett.* **88** 207208
- [41] Gross E K U and Kohn W 1985 *Phys. Rev. Lett.* **55** 2850
Gross E K U and Kohn W 1986 *Phys. Rev. Lett.* **57** 923 (erratum)
- [42] Ullrich C A and Flatté M E 2002 *Phys. Rev. B* **66** 205305
- [43] Marder M P 2000 *Condensed Matter Physics* (New York: Wiley)